CHAPTER 4

RESULTS AND DISCUSSION

The effect of crosslinking agent on morphologies of copolymer was the first parameter studied. It was done by using SPG membrane with a pore size 1.42 μm. The polymerization recipe and experimental results are summarized in Table 1 and classified based on the preparation with and without the crosslinking agents.

4.1 Effect of crosslinking agent

4.1.1 Non-crosslinked poly(styrene-co-MMA) microspheres

In Table 4.1, the formulations which yielded uniform microspheres of poly(styrene-co-MMA) having tiny holes are summarized. In Run 106, the dispersion phase containing 80:20 weight ratio of St-MMA, the particles having two small uniform holes were obtained. Corresponding to Run 108, the dispersion phase containing 50:50 weight ratio of St-MMA, the particles with a large uniform hole were also obtained. All the copolymers were prepared with hexadecane (HD) as additive. These St-MMA copolymeric spheres possessed holes created by the phase separation of hydrophobic HD. These phenomena are caused by the process of forming the spheres. The hydrophobic additive began to separate the main domain inside the sphere from the early stage of polymerization. After the reaction was complete, the additive was partially trapped inside the voids or between the polymer chains of the non-crosslinked spheres. In treatment of the spheres by an extraction with methanol, the solvent removed the unreacted comonomers or additive from the spheres. Thus, the spheres with holes were obtained. SEM photographs of these spheres are shown in Figure 4.1

4.1.2 Synthesis of solid uniform crosslinked poly(styrene-co-MMA) microspheres

The polymerization recipe and experimental results are summarized in Table 4.1. Crosslinking agent; divinylbenzene (DVB) and ethyleneglycol dimethacrylate

(EGDMA) required to give monodisperse crosslinked particles by St-MMA copolymers using the recipe given in Table 4.1 with an SPG pore size of 1.42 μm. Nitrogen pressure was applied for each run at 0.325 Kgf/cm^2

When the crosslinking agent DVB at a concentration 6.67 wt% based on the monomer was added in Run 107, and EGDMA with various concentrations of 10, 20, 42 wt% based on the monomer was added in St-MMA copolymers Runs 110, 111, and 113, respectively. As shown in SEM photographs in Figure 4.2, nonspherical particles were obtained.

4.1.2.1 Phase separation in lightly crosslinked networks

In free radical polymerization, the polymeric radicals were generated by the radical initiator. The living radicals at the end of a main-chain and the living radicals in the pendant group will form a branch chain. Also in the case of termination by the combination process, gelation is predicted to occur; and this process will form an interlinking between polymer radicals, as shown in Figure 4.3

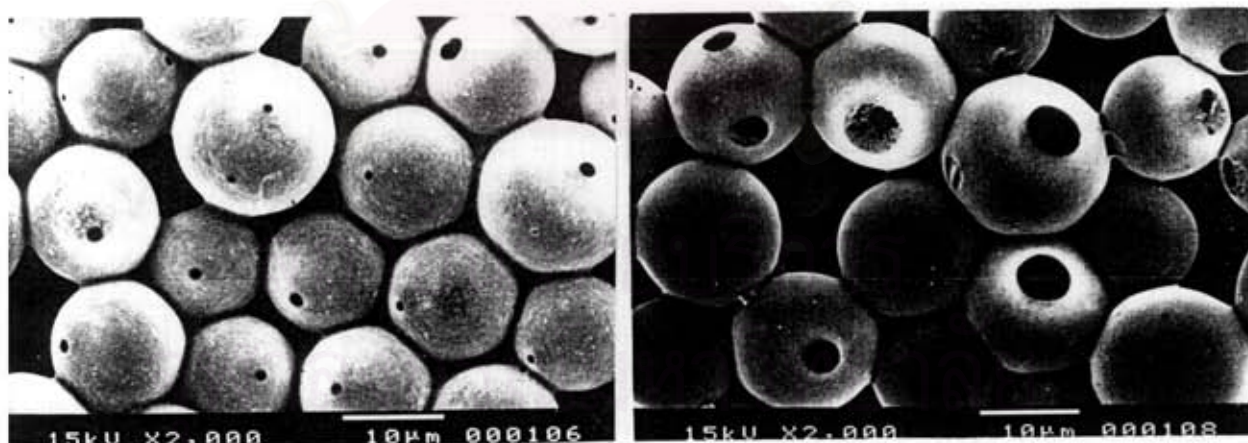a) Run 106   b) Run 108

Figure 4.1 SEM photographs of non-crosslinked poly(styrene-co-MMA) particles; St/MMA; a) 80:20 wt% ratio and b) 50:50 wt% ratio in monomer feed

Table 4.1 Polymerization recipe of poly(styrene-co-MMA) and experimental results with and without crosslinking agent using SPG pore size 1.42 μm

Run No.	106	108	107	110	111	113
Dispersion phase						
Styrene (g)	12.80	8.00	7.50	7.27	6.67	5.60
MMA (g)	3.20	8.00	7.50	7.27	6.67	5.60
DVB (g)	0	0	1.00	0	0	0
EGDMA (g)	0	0	0	1.46	2.66	4.80
Hexadecane (g)	1.50	1.50	1.50	1.50	1.50	1.50
BPO (g)	0.45	0.45	0.45	0.45	0.45	0.45
Results						
Emulsion droplets						
$\overline{D}_e$ (μm)	14.75	15.26	16.17	13.66	8.58	9.74
σ (μm)	2.02	2.08	2.53	1.62	1.22	1.37
CV (%)	13.70	13.60	15.65	11.83	14.26	14.02
Polymer particles						
$\overline{D}_p$ (μm)	12.56	13.14	13.67	12.95	7.04	8.85
σ (μm)	1.80	2.50	3.87	2.22	0.96	1.17
CV (%)	16.43	19.02	28.50	17.13	13.61	13.26
Conversion (%)	63.49	70.26	80.75	89.73	73.40	84.45

Continuous phase: H_2O 230 g, PVA-217 1.50 g, SLS 0.04 g, Na_2SO_4 0.05 g, and hydroquinone 0.016 g
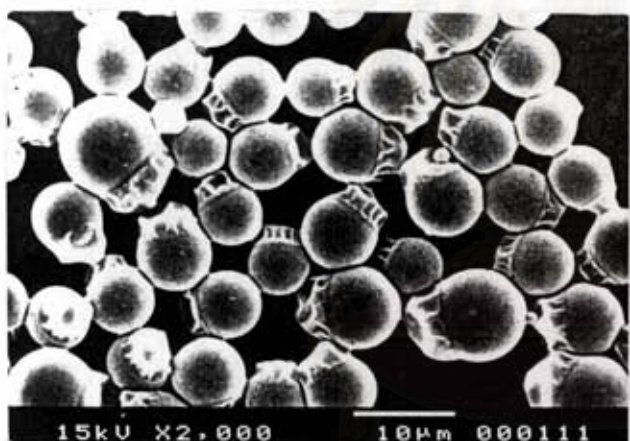
a) Run 107
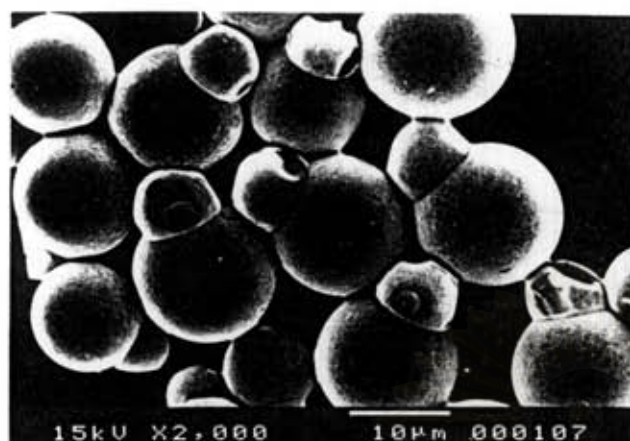
b) Run 110
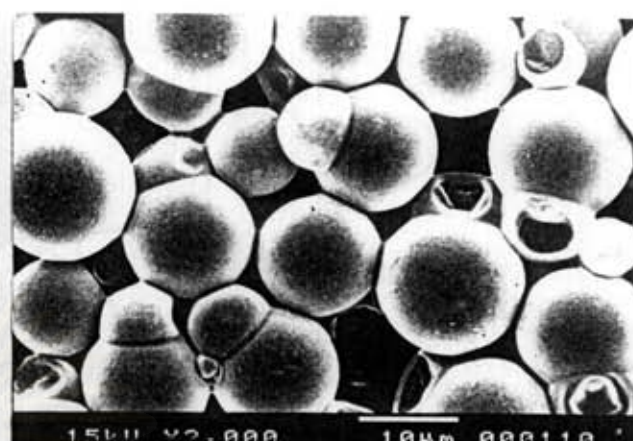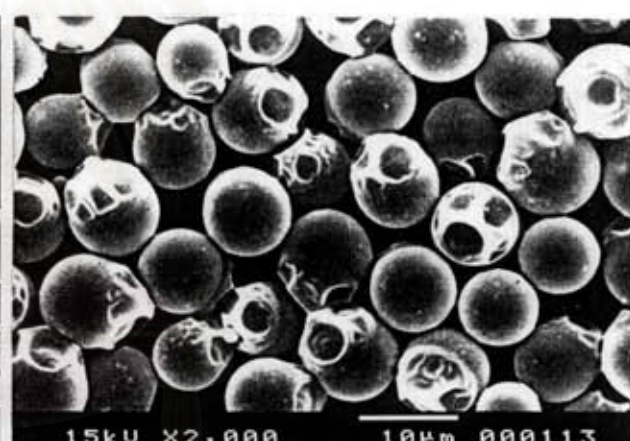

c) Run 111

d) Run 113

Figure 4.2 SEM photographs of crosslinked poly(styrene-co-MMA) particles:
a) DVB 6.67 wt%, b) EGDMA 10 wt%, c) EGDMA 20 wt%, and d) EGDMA
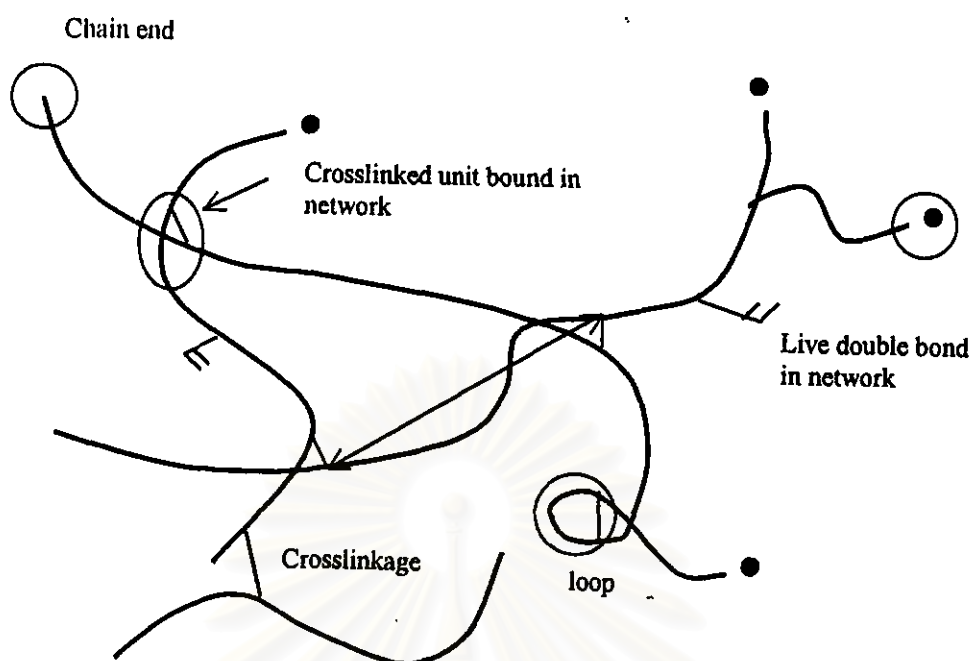42 wt% of monomer in the feed, respectively.

Chain end

Crosslinked unit bound in
network

Live double bond
in network

Crosslinkage

loop

Figure 4.3 Schematic drawing of crosslinked polymer network synthesized during free-radical polymerization [35]

The addition of crosslinking agent was expected to decrease the phase separation and to produce the spherical microspheres. However, an apparent phase separation was observed. Such phenomenon suggested that the difference in propagation rate of styrene, methyl methacrylate, and crosslinking agent (DVB or EGDMA) radicals may attribute to the phase separation. EGDMA rich copolymer composed of $-COOCH_3$ pendant groups were formed in the early stage of the polymerization; DVB or EGDMA is more reactive than styrene and will tend to be consumed earlier. The reaction of EGDMA formed the nuclei of crosslinked copolymer. When the monomer mixture contains a crosslinking agent, the crosslinked copolymer becomes insoluble in the monomer and hydrophobic additive. The phase separation occurs between styrene-rich phase and MMA-rich phase and yields hemisphere particles. The spherical or spheroidal particles were attributed to the crosslinked networks formed during the polymerization and the amorphous matrix, to the non-crosslinked polymer. Thus, the crosslinked polymer networks comprised both crosslinked and non-crosslinked fractions; the small amount of divinylbenzene, the spherical part were observed the crosslinked fraction and the head of snowman was the partially non-crosslinked fraction. The phase separation, which predicted also

causes from the incompatible between hydrophobic additives was investigated. Hexadecane played a role of a strongly hydrophobic additive in an emulsion process which stabilized the emulsion droplets. Hexadecane was isolated in the MMA-rich phase domain, which was formed in the later stage of polymerization. Since the microspheres contain a low degree of crosslinking, after polymerization, hexadecane was extracted by methanol in the purification process, a hole in the styrene-rich phase, the head of snowman was formed.

4.1.2.2 Phase separation in highly crosslinked networks

The highly crosslinked microspheres of St-MMA copolymer, contained the crosslinking agent of more than 20 wt% of the monomer in Runs 111 and 113, gave snowman-like morphologies. The particle surface looks harder and thicker because of the higher density of the crosslinking agent. The high degree of crosslinking would have given a tighter network. In other words, the higher the crosslink density of the particles, the smaller was the non-crosslinked fraction. As shown in Figures 4.2c, and 4.2d, the snowman-like morphologies were obtained. It is seen that an increase in the degree of crosslinking from 20 to 42% EGDMA, the size of separated phase domain becomes smaller. The particles have a good tendency to be spherical as the head of snowman is smaller, and the dimple was found instead of holes. This is because hexadecane was expelled onto the surface completely due to the high crosslinking density of EGDMA in the microspheres.

4.2 Effect of additives

Particle morphology is affected by the structure of polymer particles, in other words, strongly dependent on the density of crosslinking. Development of the phase separation with the progress of polymerization is enhanced by the incompatibilities between polymer chains and other ingredients initially added in the dispersion phase. To study this effect, the polymerization recipes were prepared as shown in Table 4.2. The N_2 pressure in the range 0.30-0.36 Kgf/cm^2 was applied.

In this polymerization system, water-insoluble or hydrophobic additives; hexadecane (HD), 1-hexadecanol (HD-OH), methyl palmitate (MP), and bees wax; white (BW), all four different types of additives behaved as an important substance on St-MMA copolymer, and revealed various phase separations depending on their hydrophobicity and molecular structure, which effected compatibility between the additives and polymer chains.

4.2.1 Effect of additives on particle sizes and particle size distribution of poly(styrene-co-MMA)

As shown in Figure 4.4, the particle size decreased with a narrow particle size distribution when hydrophobic additives were changed from long-chain alkane, hexadecane to long-chain alcohol, 1-hexadecanol, and to long-chain esters, methyl palmitate and bees wax, respectively. Considering a system of two different kinds of liquids, liquid-liquid system, one is termed as an oil phase and the other is termed as a water phase. The interfacial tension, γ is determined by the internal forces in the liquid, thus it will be related to the internal energy, as shown in Figure 4.5.
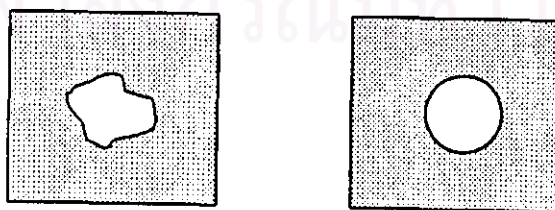

Figure 4.5 Interfacial tension causes the equilibrium in the right drawing, where the circular shape is formed [36].
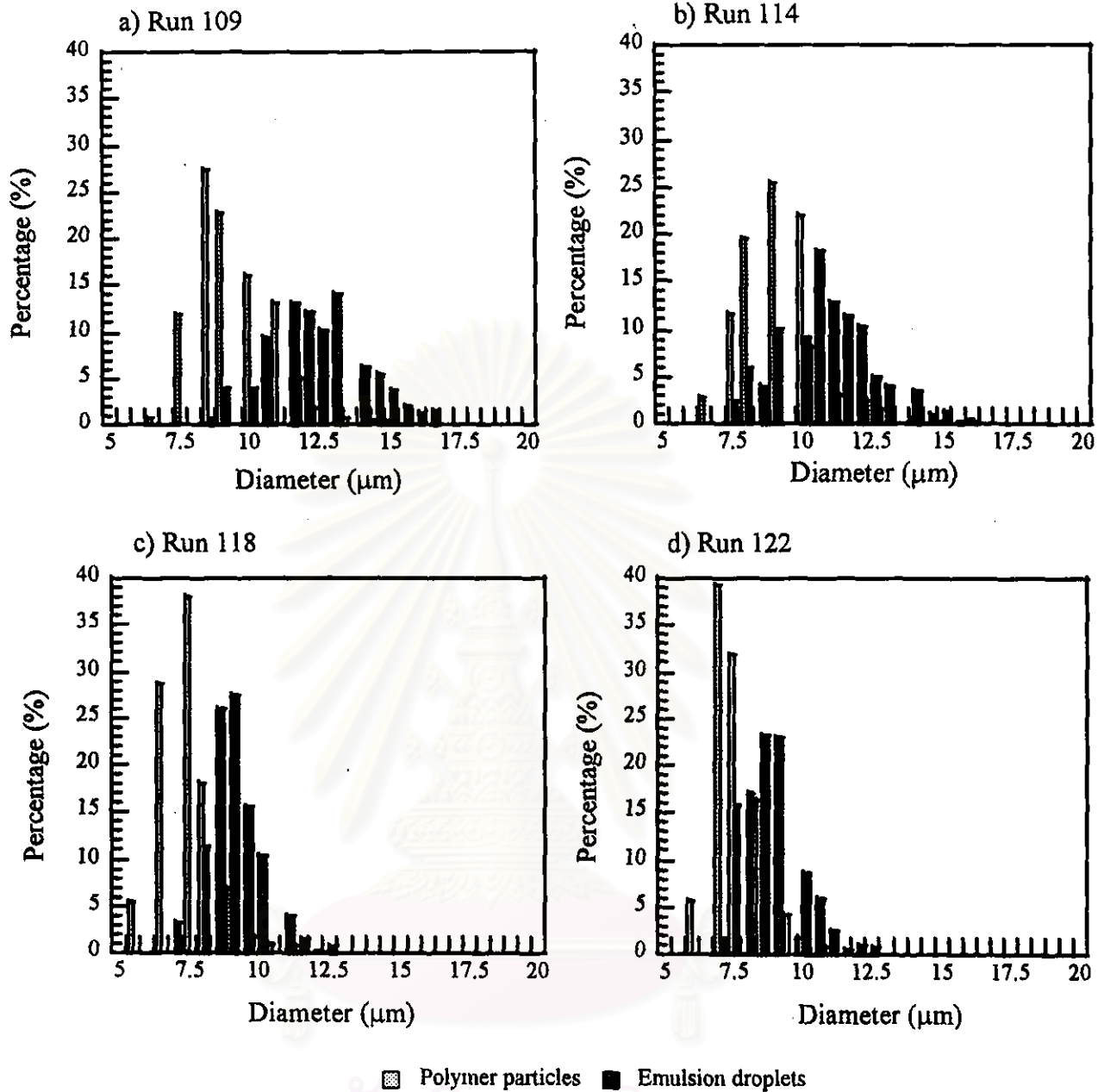
Figure 4.4 Histograms of size distribution of poly(styrene-co-MMA); Effect of additives: a) Hexadecane, b) 1-Hexadecanol, c) Methyl palmitate, and d) Bees wax, respectively.

In the synthesizes of the St-MMA copolymer without adding any additive, the experiment was carried out with a dispersion phase containing 50:50 weight ratio of St-MMA shown in Run 143. The polymer particles with a broad particle size distribution were obtained as shown in Figure 4.6. Besides the main population of the particles of 8.12 μm diameter, another population of larger particle sizes larger than 100 μm was found. The lack of additives causes a low interfacial tension between the monomer phase and the water phase. In other words, MMA monomer which is partially water-soluble (the solubility in water is 16 g/dm^3 at 298 K [37]) dissolves in water. Also, the collision of droplets occur due to the stirring force during the polymerization process. Precisely, to promote the surface area and increasing the interfacial tension, a hydrophobic additive was added with various types of functional group.

The hydrophobic additives will affect at the boundary between two phases. In case of long-chain alkane, hexadecane (16 carbons atom in the alkyl group), the molecules of the alkanes at the surface exhibit hydrophobicity, dependence on the hydrophobic chain length due to the low polarity, so that the additives may not be able to present at the aqueous phase. Therefore, HD can yield the large emulsion droplets with an average droplet diameter of 12.25 μm, and a coefficient of variation of 14.06% obtainable in Run 109.

The different homologous series provide valuable information about the stabilizing forces in fluid. 1-Hexadecanol has more polarity than HD due to the functional group of alcohol; the additive can come out to the surface of droplets and affected the interfacial tension between two phases exhibiting the lower interfacial tension due to the more affinity with water. Therefore, use of 1-hexadecanol as an additive shows that the droplet size distribution tends to be narrow and smaller emulsion droplets; an average droplet diameter of 10.85 μm was obtained in Run 114.

Methyl palmitate (MP) reveals the great compatibility with St-MMA copolymer, in particular with the MMA segment according to the suitable alkyl chain length and the influence through the functional group. The smaller droplet diameter of 8.98 μm was obtained with a narrow size distribution. The stability of droplets due to the hydrophobicity of alkyl group may enhance the compatibility with styrene, and the ester group of the additive also promoted the compatibility with the ester group of MMA. As well as the ester functional group possesses the hydrogen bonding so that

MP can come out to the surface of droplets due to the formation of hydrogen bonding. The lower the interfacial tension, the smaller the particle sizes. Then, the additive was switched from methyl palmitate to methyl laurate to evaluate the effect of chain length in the alkyl group. As such the shorter alkyl chain length of methyl laurate was used so that methyl laurate is more hydrophilic than methyl palmitate. The lower affinity with monomer may increase, in which the emulsion droplets with the average diameter 11.20 μm was obtained.

Addition of more hydrophobic additives containing long-chain alkyl groups of hydrocarbons (24 to 36 carbon atoms in the alkyl group) with the ester functional group such as bees wax, led to much more finely dispersed emulsions, and greatly increased the stability of emulsion. These are possibly resulted from higher alkyl chain lengths. The smaller droplet diameter of nearly 7 μm and a narrow droplet size distribution with a coefficient of variation of 12.11% was obtained. Furthermore, due to the higher viscosity of the dispersion phase containing bees wax, the dispersion phase with highest viscosity is difficult to permeate through the membrane, hence the droplets were formed in smaller size.
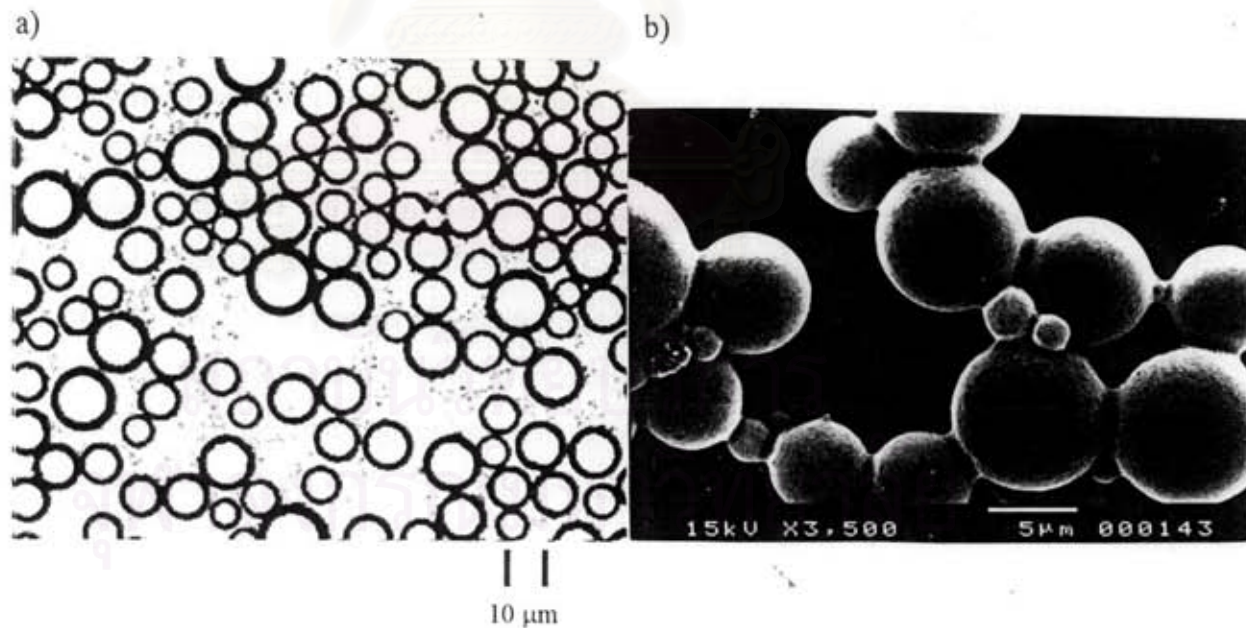

Figure 4.6 Photographs of the poly(styrene-co-MMA) in Run 143 without additive: a) Photograph of the droplets taken by an optical microscope; b) SEM photograph of the particles; CV = 20.15%, and $\overline{D}_p$ = 8.12 μm

4.2.2 Effect of various additives on morphologies

Poly(styrene-co-MMA) particles with different morphologies were obtained by SPG emulsification. The study was conducted by using four types of additive as follows: Run 109 with hexadecane, Run 114 with 1-hexadecanol, Run 118 with methyl palmitate, and Run 122 with bees wax; the concentration of additives for each run is 10 wt% based on the monomer and crosslinking agent concentrations; 5 wt% of EGDMA was added based on the monomer content. The SEM photographs are shown in Figure 4.7

In Run 109 as discussed previously on the effect of crosslinking agent, when the crosslinking network begins to develop among the growing chains of each monomer under the high interfacial tension of hexadecane and the incompatibility of Styrene and MMA. The particles might either distort in some way to account for the effect of additives. Such a deformation revealed nonspherical microspheres as a snowman-like morphology. Comparison with the added hexadecane without the crosslinking agent in Run 108, the spherical particles with a single hole were obtained. This morphology clearly supports the phase separation of hexadecane.

Changing the additive type from hexadecane to long-chain alcohol, 1-hexadecanol was done in Run 114. The same number of carbon atoms in alkyl group but different on functional group is an interest. The spherical particles with a platelet-like debris attached on each particle surface were obtained. Consideration on interfacial tension between St-MMA, St-hexadecanol, and MMA-hexadecanol, probably hydroxyl end groups of hexadecanol have an affinity with the ester group of MMA better than styrene. Also the lower interfacial tension of alcohol than alkane, 1-hexadecanol will become a good pair with MMA and it may slightly dissolve in the continuous phase. The MMA-rich phase was probably expelled to the surface and reflected in small flakes on the surface.

The spherical microspheres were prepared using methyl palmitate as an additive in Run 118. The ester group of methyl palmitate has an affinity with an ester group of MMA. Thus, the spherical shape developed.

The usage of the large molecule with higher numbers of carbon atoms ranging from 24-36 atoms (not clearly indicated by the supplier) was carried on in Run 122. The nonspherical particles were obtained. As described in the previous Section of 4.2.1, the particles containing bees wax revealed a smaller average size with a narrow

size distribution, probably due to that the long chain alkyl has a higher affinity with styrene and MMA. However, the snowman-like microspheres were obtained. Consequently, the crosslinking agent pushed out the bees wax during the crosslinking reaction. Also, the MMA rich copolymers moved with bees wax because of the higher affinity with than the additive containing the hydroxyl group as functional group; the platelets in Figure 4.7b changed to the solid 'head' of the hemisphere in Figure 4.7d. Thus, the wax remains on the particle surface. The FT-IR spectrum reveals broad band of ester group in range 2500-3600 cm^{-1} (see Appendix E-1d; FT-IR spectrum in Run 122).

4.2.3 Effect of composition of hydrophobic additives

Poly(styrene-co-MMA) particles synthesized using different types of the additive revealed that the particles size decreased with a narrow size distribution when the additives were changed from hexadecane to 1-hexadecanol to methyl palmitate and to bees wax, respectively. For comparison, the mixed additives were studied. The experimental recipe and results are shown in Table 4.2. To determine the effect of composition of the additives, two different types of the additives (X/Y) were mixed into the dispersion phase at the weight ratios of 25:75, 50:50, 75:25, and 10%, based on the monomer concentration.

4.2.3.1 Average diameter of poly(styrene-co-MMA) particles

Figure 4.8 shows the relationship between the average diameter of particles and the fraction of a particular additive. In the mixture of hexadecane and 1-hexadecanol, the smaller polymer particles are obtained when the mixture contains 25 wt% of hexadecane in Run 117. An average particle diameter of 7.81 µm was obtained. Since the molecules of the alkanes at the surface may exhibit some interesting phenomenon dependence on the chain length, which can be related to van der Waals interaction between chains. However, it is quite weak interaction. Whilst, the alcohols would be mainly stabilized by both van der Waals force and hydrogen bonds [36], the latter being stronger than the former. The molecule arrangement of HD and 1-hexadecanol (HD-OH) in this composition dominantly reveal the effect of

HD-OH at the droplet surface more than that of HD. The smaller droplets were thus obtained. Whereas, Run 116 with the mixture of 50 wt% of HD, an average particle size diameter of 9.11 μm was obtained. The composition may not be possibly a favorable ratio for the additives. However, the particles size increased and became close to that obtained with 100% 1-hexadecanol as the amount of 1-hexadecanol is higher. The particles prepared using the mixed additives between hexadecane and methyl palmitate clearly showed the effectiveness of the change of interfacial tension due to the presence of additives. The particle size decreased with increasing amount of methyl palmitate. In Run 120, the emulsion droplets with a diameter of 6.84 μm with a narrow size distribution and a coefficient of variation of 10.41% were obtained.

The mixed additives of the same functional group was done using methyl palmitate and bees wax. When the mixture contains 50% of bees wax in Run 123, and 25% of bees wax in Run 124, an average particle size of 8.80 and 6.34 μm, respectively, were obtained. The smaller size compared with the mixed additive containing the other functional groups of alkane or alcohol is reduced to the interaction between hydrogen bonding of the ester groups.

El-Aasser et al., in their miniemulsion polymerization of styrene, claimed that the highest number of polymer particles and the solid emulsion were obtained when a 1:3 molar ratio of SLS and hexadecanol was employed. Yuyama et al. [38] reported the very complex behavior of the interfacial tension between the droplets and the continuous phase when they employed PVA and SLS as a mixed stabilizer in the aqueous phase, and used hexadecane as a hydrophobic additive in their emulsion of styrene and DVB.

The results of the present system are, by no means, not directly comparable with their results, however, it can be said that the complex behavior of droplet size in Figure 4.8 is certainly due to the complex formation of the two additives on the interface between the droplets and the aqueous phase.

4.2.3.2 Morphologies of poly(styrene-co-MMA) particles

To determine the effects of functional group and polarity, the mixture of hexadecane and 1-hexadecanol was studied. The ratios of HD/HD-OH are 50:50 and 75:25 for Runs 116 and 117, respectively. The polymer particles reveal dual

morphologies one of which has a trace of circular area on the surface, and the other forms spheres with some debris. Furthermore, the small-sized particles of about 1 μm also formed. Consequently, on the hydrophobicity of hexadecane, HD is mixed with a more polar additive so that the amount of polymer in the domain is not enough to form filmy skin which bursted out in extraction process. However, if the amount of hexadecane is higher, the morphology shifts to the hemisphere particles, and only the phase separation of hexadecane on the surface was observed.

The homogeneous spheres were obtained using methyl palmitate as a co-additive. The ratio of HD/MP was selected at 50:50 and 25:75 in Runs 119 and 120, respectively. Similarly with the results in Run 116, the trace of circular area on the surface is also present in Run 119 when the 50% of HD were used. After decreasing the amount of HD to 25%, the particles showed very tiny holes resulting from the phase separation of HD. Therefore, MP is more dominant in forming the holes than HD when the amount of MP is higher than 50%.

The mixtures of methyl palmitate and bees wax were studied at the ratios of MP/BW 50:50 and 75:25 in Runs 123 and 124, respectively. Bees wax is more dominant on morphologies in the two runs than MP. The compatibility of MP with St- and MMA-rich phase developed the spherical domain; whereas, bees wax, the long chains ester with higher affinity than the low molecular weight ester in which the phase separation may enhance in the MMA-rich phase. The snowman-like morphology was obtained in both Runs. SEM photographs for each run were shown in Figures 4.9 and 4.10.

Table 4.2 Polymerization recipe and experimental results of poly(styrene-co-MMA) with various hydrophobic additives using SPG pore size of 1.42 μm

Run No.	109	114	116	117	118	119	120	121	122	123	124
Dispersion phase											
Styrene (g)	7.50	7.60	7.62	7.62	7.62	7.62	7.62	7.62	7.62	7.62	7.62
MMA (g)	7.50	7.60	7.62	7.62	7.62	7.62	7.62	7.62	7.62	7.62	7.62
EGDMA (g)	0.76	0.76	0.76	0.76	0.76	0.76	0.76	0.76	0.76	0.76	0.76
Hexadecane (g)	1.50	0	0.75	1.12	0	0.75	0.38	0	0	0	0
1-Hexadecanol (g)	0	1.50	0.75	0.38	0	0	0	0.75	0	0	0
Methyl Palmitate (g)	0	0	0	0	1.50	0.75	1.12	0.75	0	0.75	1.12
Bees wax (g)	0	0	0	0	0	0	0	0	1.50	0.75	0.38
BPO (g)	0.45	0.45	0.45	0.45	0.45	0.45	0.45	0.45	0.45	0.45	0.45
Results											
Emulsion droplets											
$\overline{D}_e$ (μm)	12.25	10.85	10.97	9.28	8.98	9.43	8.41	10.61	8.84	9.92	6.77
σ (μm)	1.72	1.74	1.49	1.24	0.97	2.42	0.88	1.59	1.07	1.47	0.70
CV (%)	14.06	16.04	13.82	13.40	10.81	25.69	10.41	15.04	12.11	14.78	10.27
Polymer particles											
$\overline{D}_p$ (μm)	9.46	9.18	9.11	7.81	7.38	7.96	6.83	9.10	7.54	8.80	6.34
σ (μm)	1.58	1.67	1.23	1.13	1.05	1.72	1.02	1.50	0.88	1.43	0.76
CV (%)	19.02	18.21	13.50	14.46	14.23	21.65	14.87	11.70	11.70	16.20	12.05
Conversion (%)	53.31	86.33	88.10	43.43	74.33	56.36	55.57	63.50	63.50	50.85	56.55

Continuous Phase: H₂O 230 g, PVA-217 1.50 g, SLS 0.04 g, Na₂SO₄ 0.05 g, and hydroquinone 0.016 g.
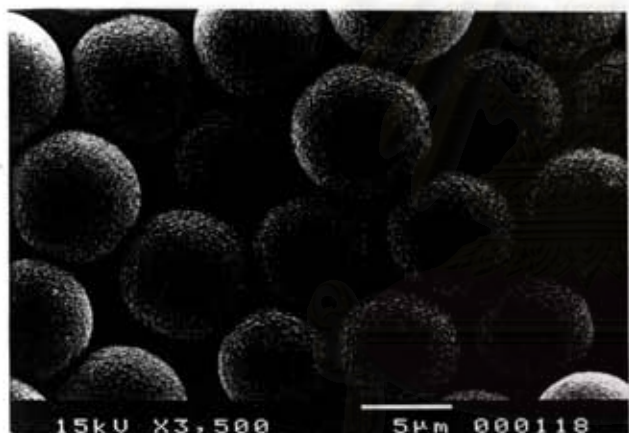
44

a) Run 109
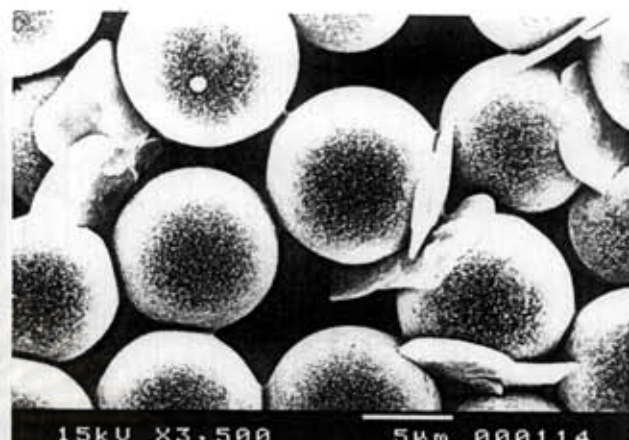
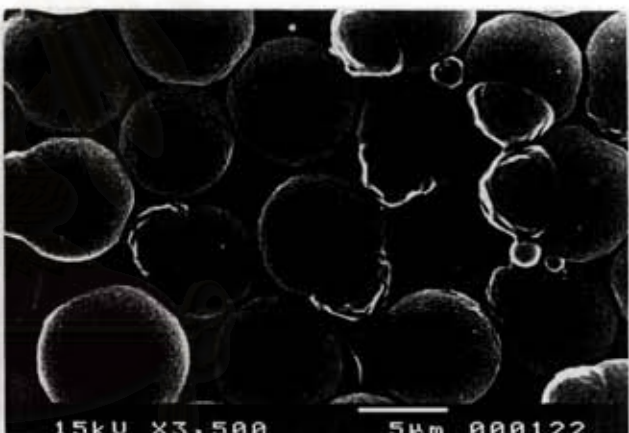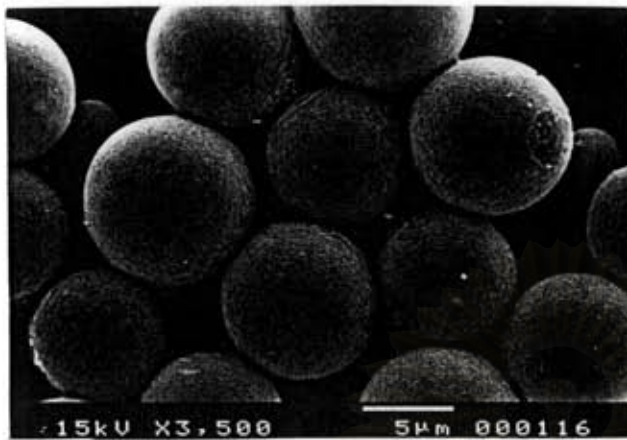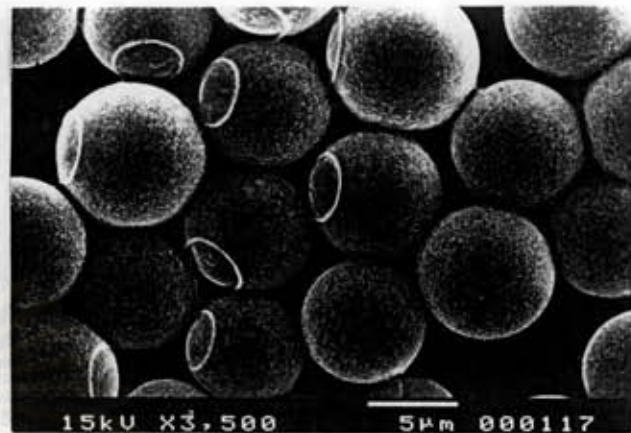b) Run 114

c) Run 118

d) Run 122

Figure 4.7 SEM photographs of poly(styrene-co-MMA) particles by various additives: a) Hexadecane, b) 1-Hexadecanol, c) Methyl palmitate, and d) Bees wax, respectively.
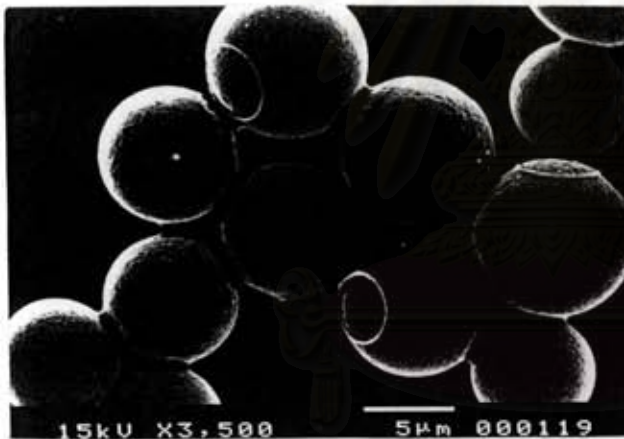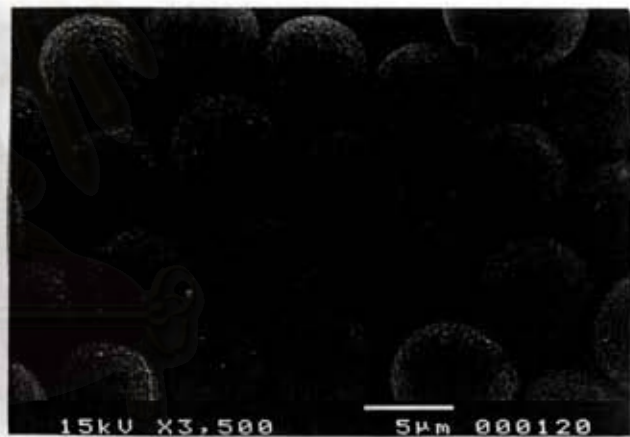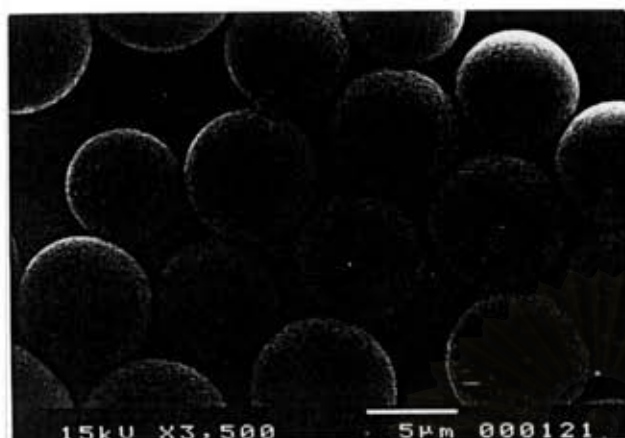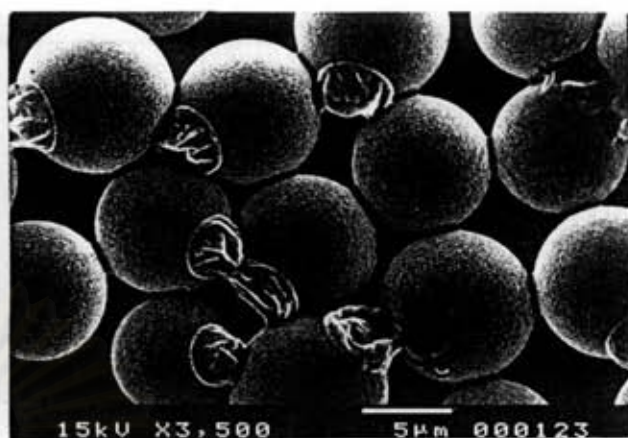
a) Run 116

b) Run 117

c) Run 119

d) Run 120

Figure 4.9 SEM photographs of poly(styrene-co-MMA) particles by various compositions of additives: a) HD/(HD-OH) 50:50 wt% ratio, b) HD/(HD-OH) 25:75 wt% ratio, c) HD/MP 50:50 wt% ratio, and d) HD/MP 25:75 wt% ratio, respectively.

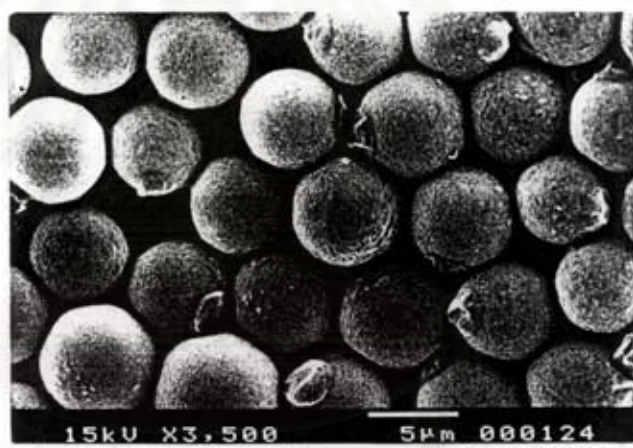a) Run 121　　　　　　　　　　　b) Run 123

c) Run 124

Figure 4.10 SEM photographs of poly(styrene-co-MMA) particles by various compositions of additives: a) (HD-OH)/MP 50:50 wt% ratio, b) MP/BW 50:50 wt% ratio, and c) MP/BW 75:25 wt% ratio, respectively.
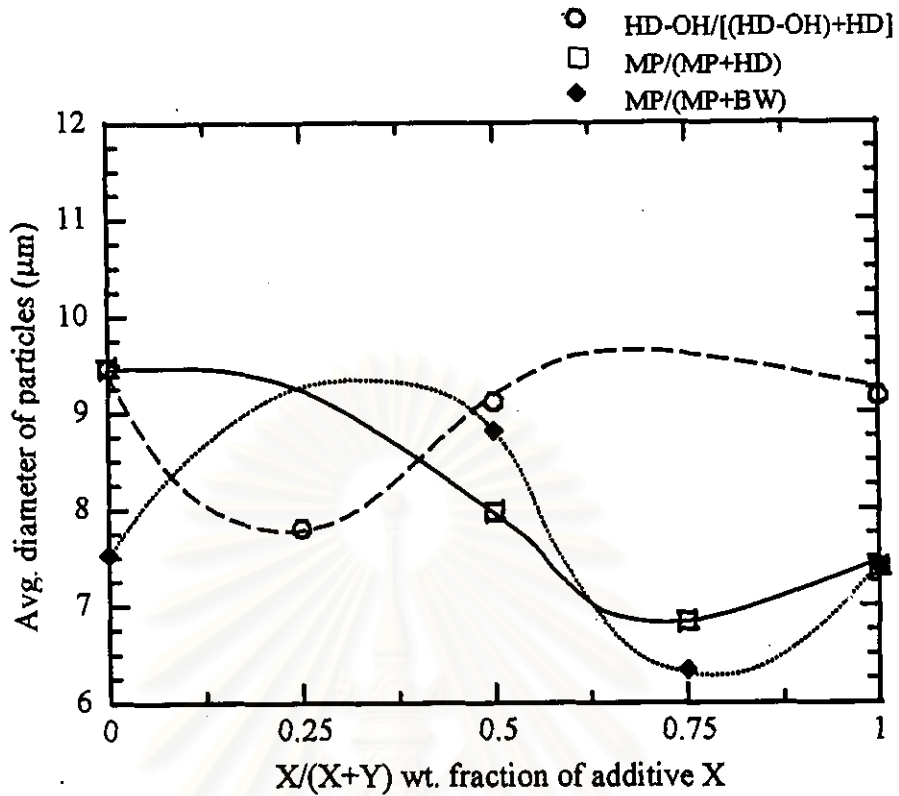
Figure 4.8 Average diameter of polymer particles with various compositions of hydrophobic additives

In summary, in the preparation of poly(styrene-co-MMA) particles, the morphologies of particles can be classified as shown in Figure 4.11
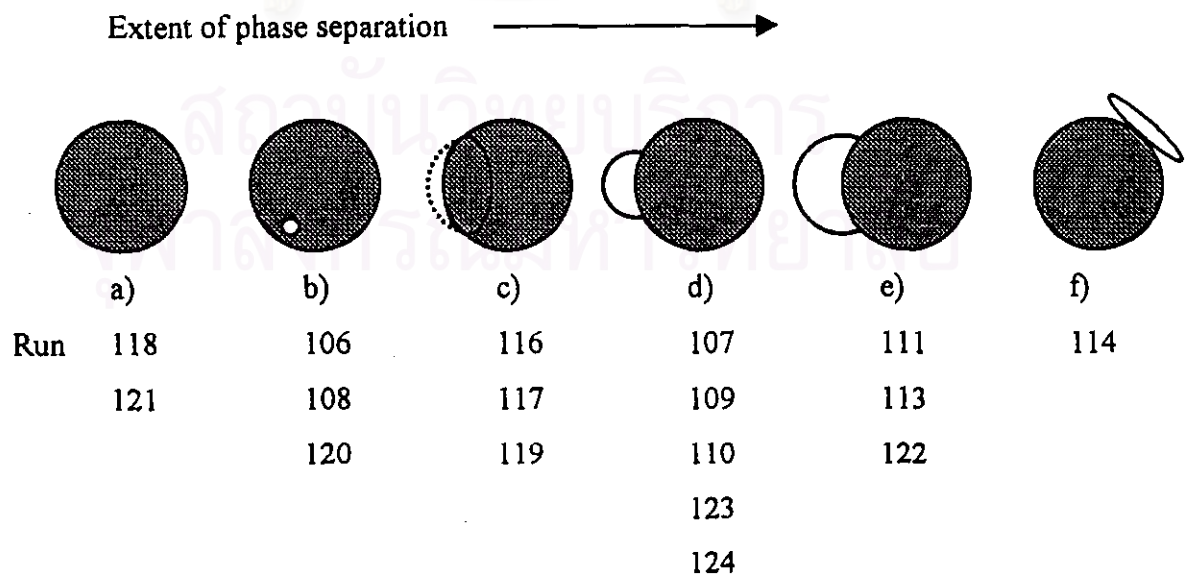

Extent of phase separation

	a)	b)	c)	d)	e)	f)
Run	118	106	116	107	111	114
	121	108	117	109	113	
		120	119	110	122	
				123		
				124		

Figure 4.11 Schematic diagram for the morphology classification in the preparation of poly(styrene-co-MMA), the wt% ratio of St/MMA in the feed of 50:50

4.2.4 Effect of additive on particle size and size distribution of poly(styrene-co-n-BMA) and poly(styrene-co-2-EHMA) particles

The preparative condition and results are shown in Table 4.3 and Figure 4.12 and 4.13. The emulsion droplets and polymer particles varied with various additives, and the size decreases from hexadecane to 1-hexadecanol, to methyl palmitate, and to bees wax, respectively. The particles size distribution of both St-n-BMA and St-2-EHMA copolymer particles revealed the similar behavior of interfacial tension as discussed in the St-MMA copolymer particles in Section 4.2.1. The exception is in case of bees wax which resulted in broad distribution, probably because of the very slow droplet protrusion through the SPG membrane. Consideration on the molecular structure of n-BMA and 2-EHMA, both monomers have a large side chain; $-COOC_4H_9$ and $-COOCH_2CH(CH_2CH_3)(CH_2)_3CH_3$, respectively. The dispersion phase of high viscosity is more difficult to permeate through the membrane. Furthermore, the hydrophobic alkyl group of bees wax does not dissolve in the water. Thus, the wax may plug up the membrane pores. The emulsion droplets become smaller when the SPG emulsification takes long time. As a result, a broad particle size distribution was resulted.

4.2.5 Effect of additive on morphologies of poly(styrene-co-n-BMA) and poly(styrene-co-2-EHMA) particles

The effect of the additives on the morphologies of different monomers was carried out employing the dispersion phase containing 50:50 weight ratio of St-n-BMA and St-2-EHMA. In order to evaluate the effect of additives on a series of alkyl methacrylate. The non-crosslinked polymers were prepared in which the experimental recipe and results are shown in Table 4.3 and Figures 4.14 and 4.15.

In Run 401, St-n-BMA particles retained a smooth skin and spherical in shape but with the small dimples observed when hexadecane was added. On the other hand, the effect of HD on St-n-BMA is similar to the case in St-MMA copolymer particles in Runs 106 and 108. n-BMA is more hydrophobic than MMA due to the long alkyl group of side chain. The side chain of n-BMA can be partially compatible with HD due to the hydrophobicity. However, the trace amount of HD was expelled to the surface and simply could be extracted by methanol to yields the dimples on the

surface. However, switching monomer to 2-EHMA, the dimples were not observed. The particle distortion of the spherical shape occurred because the monomer yields a lower glass transition temperature than does n-BMA. Thus, the St-2-EHMA particles have more soft and rubbery-like morphology, unable to keep the spherical shape. The hemisphere and flatten particles which sticking together can be observed on the SEM photographs in Figures 4.14a, and 4.15a.

St-n-BMA and St-2-EHMA copolymer particles prepared by 1-hexadecanol still showed the phase separation. The spherically shape particles with some platelet-like debris morphologies were obtained. The number of the debris on both copolymer particles increased more than those observed in St-MMA particles. The increase of separated domains suggested an improved compatibility of 1-hexadecanol with the monomers since they are more hydrophobic than MMA.

Methyl palmitate still revealed great compatibility, yielding the spherical shape of St-n-BMA and St-2-EHMA copolymer particles. However, both particles stuck together and deformed due to the low Tg copolymers. Bees wax represented the good additive in the synthesis of the St-n-BMA and St-2-EHMA copolymer. The small flakes on the surface may suggest the partial phase separation of bees wax with a small amount of the polymer when bees wax was expelled to the surface.

To do the characterization of polymer, molecular weight, molecular weight distribution, and thermal properties were examined. The results are shown in Table 4.4, and Figures 4.16 and 4.17. In the series of St-n-BMA copolymer, as the ratio of styrene/n-BMA is 50:50 wt% ratio, the same range of molecular weight was obtained. All copolymers have the narrow molecular weight distribution, and a unimodal molecular distribution curve was obtained. The thermal property measurement revealed the two values of Tg in St-n-BMA copolymer series. Clearly, the copolymer of different compositions was formed, one is a fraction of a polymer containing the hard segment of phenyl pendant group of styrene as represented in Tg_2, and the other is rubbery segment corresponding to rubbery structure of the side chain of n-BMA as represented in Tg_1. The calculated Tg, based on Fox equation (see Appendix B), and the Tg_2 from the measurement are close to Tg, the Tg_1 corresponds to the Tg of n-BMA homopolymer (293 K). Precisely, the polymer having the Tg_2 revealed the copolymer of St and n-BMA. The single Tg value of St-2-EHMA copolymer disclosed the similar result from the calculated values, possibly due to the good compatibility between the two copolymers with different appearances. However, the

transition signals are broad for all St-2-EHMA samples as in the process of precipitation, the phase separation was observed, the precipitants are more viscous and distinguishable into two layer; one is the polymer powder and the other is transparent and tough like a rubber.

Table 4.4 Characterization of poly(styrene-co-n-BMA) and poly(styrene-co-2-EHMA); the feed composing 50:50 weight% ratio of St-n-BMA and St-2-EHMA

Run No.	$\overline{M}_n$	$\overline{M}_w$	$\overline{M}_w / \overline{M}_n$	$T_{g(calc)}$, K	$T_{g1(obs)}$, K	$T_{g2(obs)}$, K
401	21970	47950	2.26	328.2	289.2	314.3
403	24800	53140	2.14	328.2	285.2	320.0
404	22080	46760	2.12	328.2	291.4	-
406	29950	54610	1.82	328.2	286.8	316.3
601	26300	60070	2.28	308.5	295.7	-
603	11450	47760	2.14	308.5	291.5	-
604	19030	50200	2.64	308.5	291.5	-
606	25220	48740	1.93	308.5	290.1	-

Table 4.3 Polymerization recipe and experimental results of poly(styrene-co-n-BMA) and poly(styrene-co-2-EHMA) with various hydrophobic additives using SPG pore size 1.42 μm

Run No.	401	403	404	406	601	603	604	606
Dispersion phase								
Styrene (g)	8.00	8.00	8.00	8.00	8.00	8.00	8.00	8.00
n-BMA (g)	8.00	8.00	8.00	8.00	0	0	0	0
2-EHMA (g)	0	0	0	0	8.00	8.00	8.00	8.00
Hexadecane (g)	1.50	0	0	0	1.50	0	0	0
1-Hexadecanol (g)	0	1.50	0	0	0	1.50	0	0
Methyl palmitate (g)	0	0	1.50	0	0	0	1.50	0
Bees wax (g)	0	0	0	1.50	0	0	0	1.50
BPO (g)	0.45	0.45	0.45	0.45	0.45	0.45	0.45	0.45
Results								
Emulsion droplets								
$\overline{D}_e$ (μm)	10.92	12.59	11.46	12.70	13.24	11.64	12.30	12.65
σ (μm)	1.13	1.59	1.43	1.54	1.78	1.28	1.32	1.81
CV (%)	10.32	12.61	12.48	12.13	13.43	10.97	10.70	14.32
Polymer particles								
$\overline{D}_P$ (μm)	9.64	10.82	9.48	10.60	13.06	10.21	10.84	10.15
σ (μm)	1.29	1.54	1.32	1.50	2.38	1.45	1.55	1.77
CV (%)	13.38	14.23	13.94	14.15	18.25	14.17	14.25	17.47
Conversion (%)	71.60	72.30	54.36	96.66	67.69	64.01	73.84	49.19

Continuous phase H_2O 230 g, PVA-217 1.50 g, SLS 0.04 g, Na_2SO_4 0.05 g, and hydroquinone 0.016 g
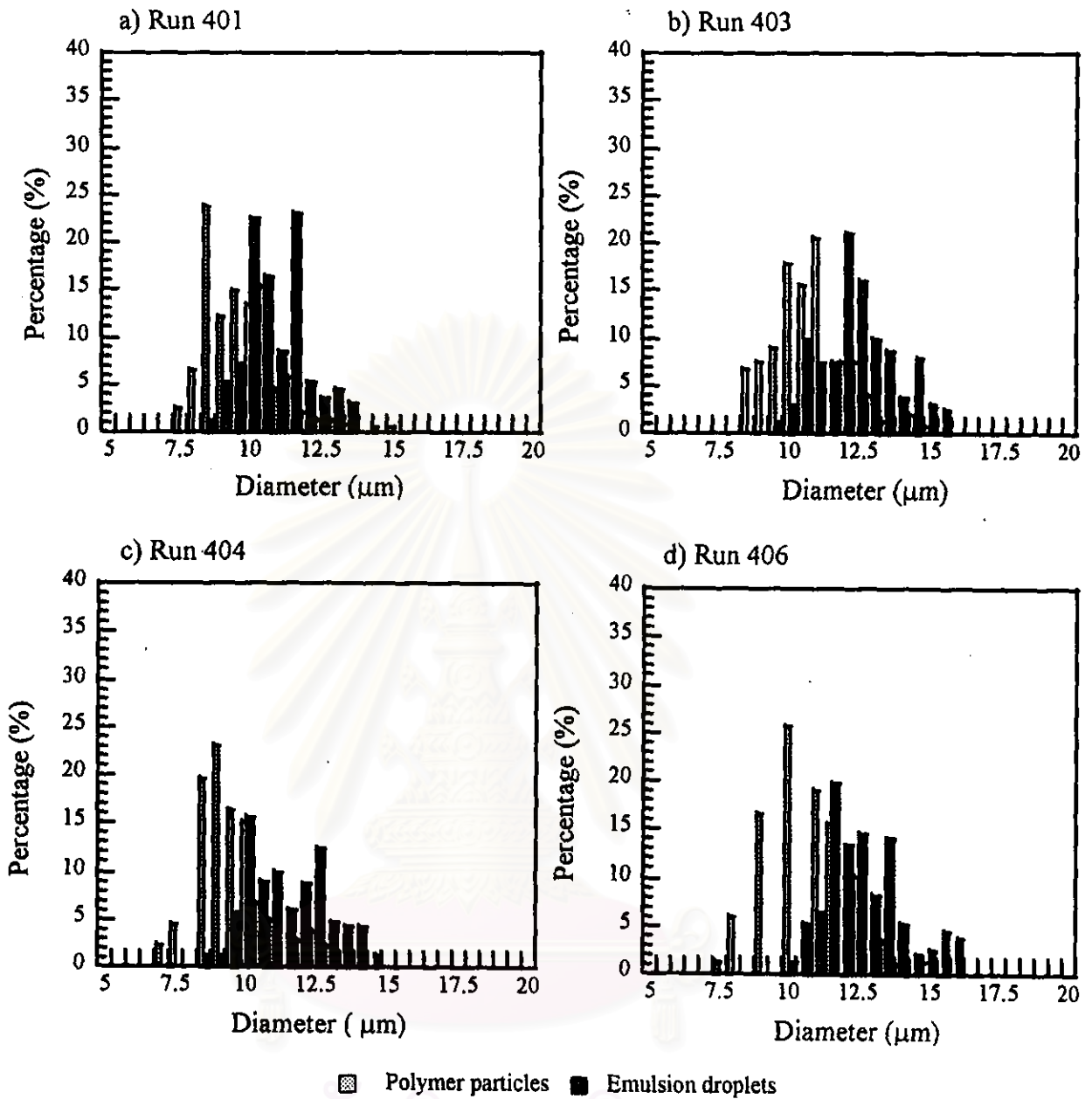
Figure 4.12 Histograms of the size distribution; emulsion droplets and polymer particles; Effect of additives on St-n-BMA copolymer: a) Hexadecane, b) 1-Hexadecanol, c) Methyl palmitate, and d) Bees wax, respectively.
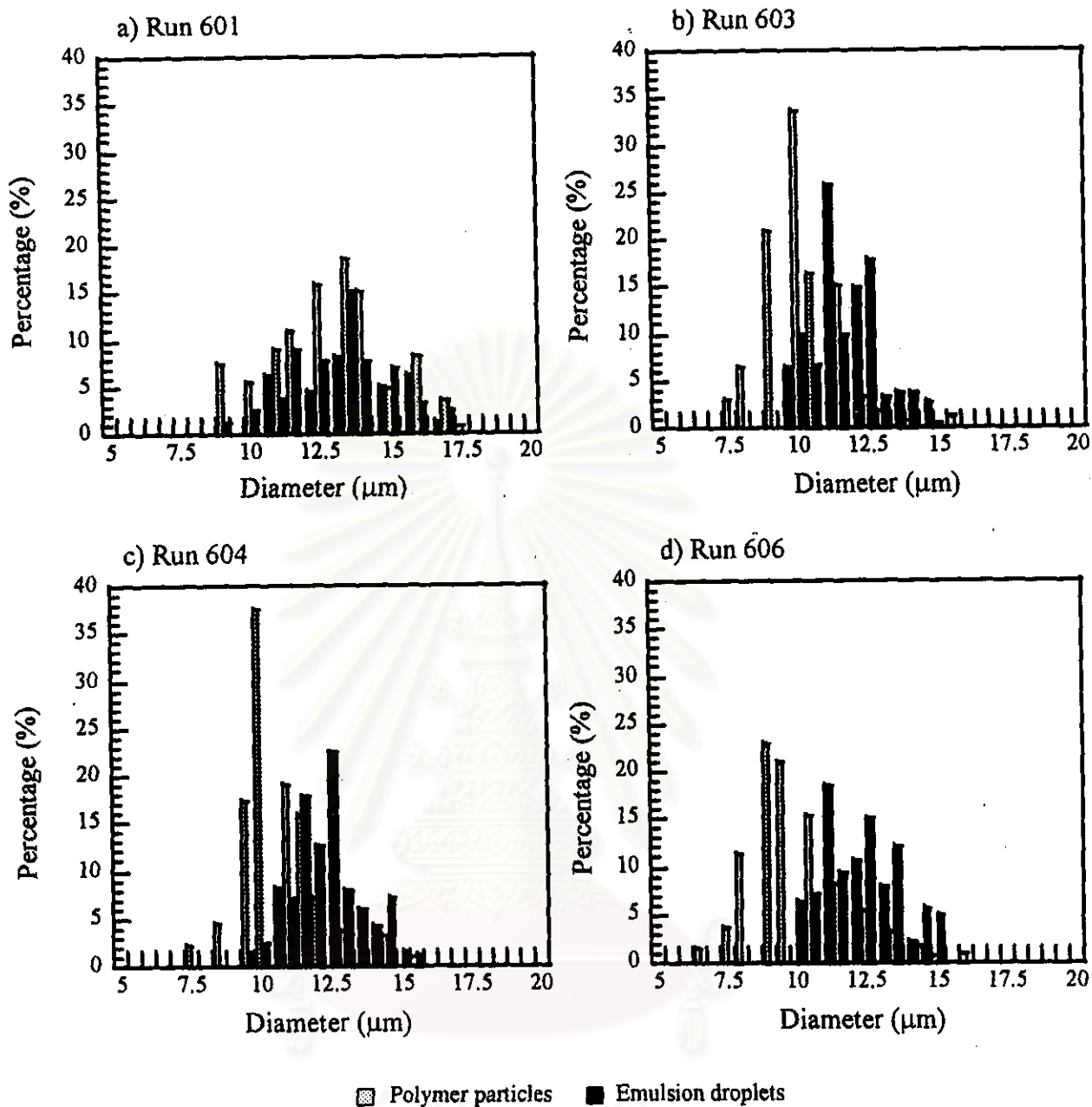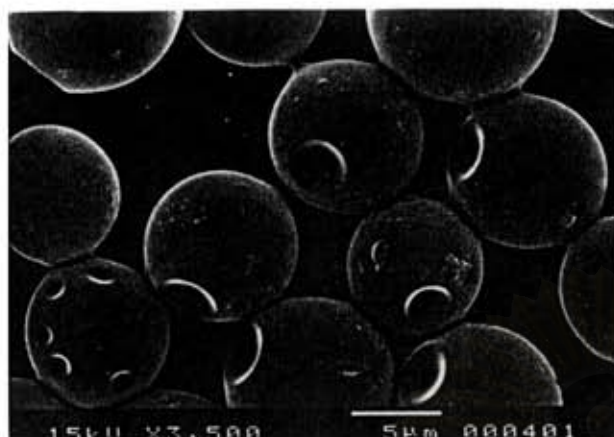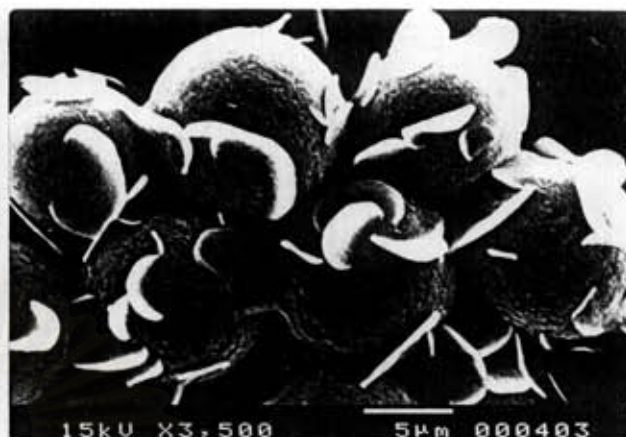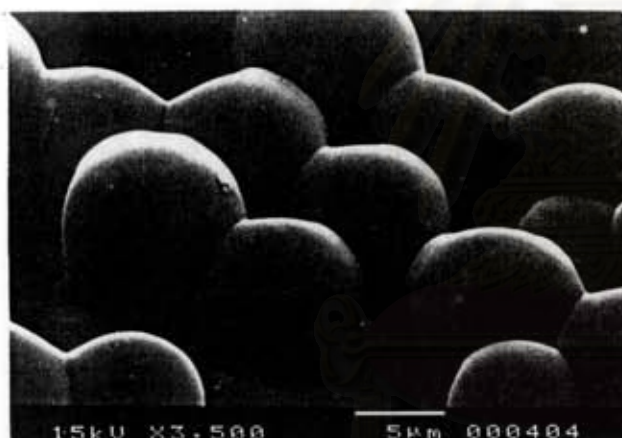
Figure 4.13 Histograms of the size distribution; emulsion droplets and polymer particles; Effect of additives on St-2-EHMA copolymer: a) Hexadecane, b) 1-Hexadecanol, c) Methyl palmitate, and d) Bees wax, respectively.
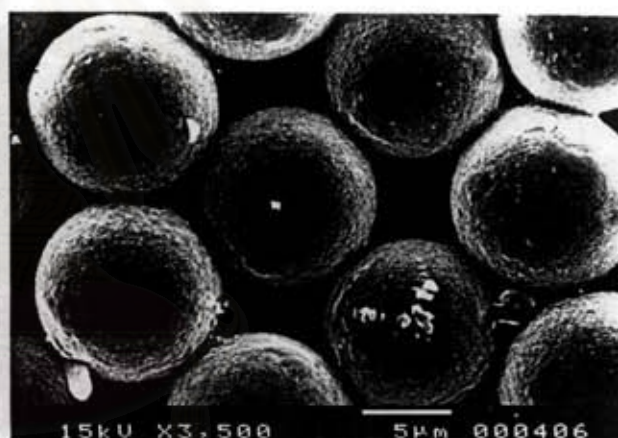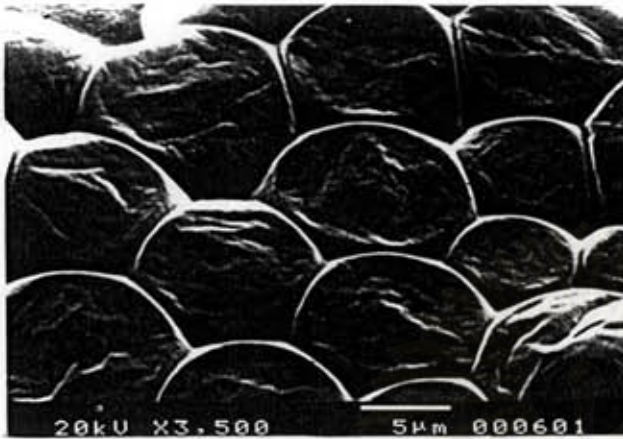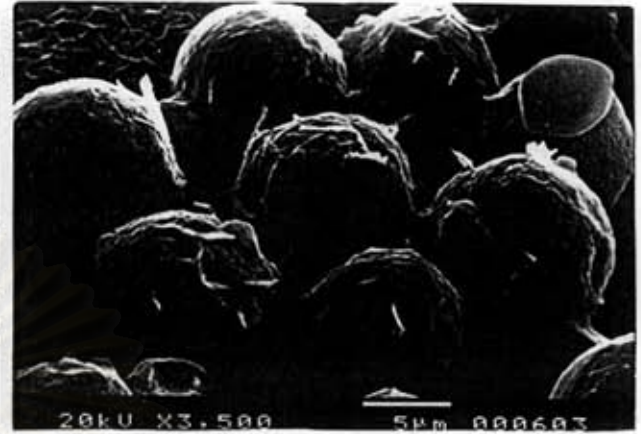
a) Run 401

b) Run 403

c) Run 404

d) Run 406

Figure 4.14 SEM photographs of poly(styrene-co-n-BMA) particles by various additives; a) Hexadecane, b) 1-Hexadecanol, c) Methyl palmitate, and d) Bees wax, respectively.

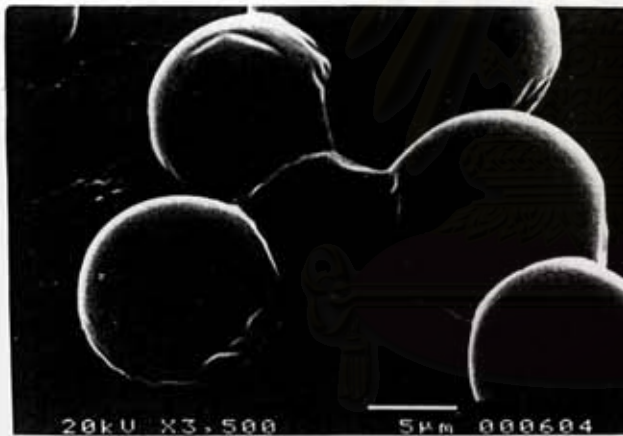a) Run 601   b) Run 603
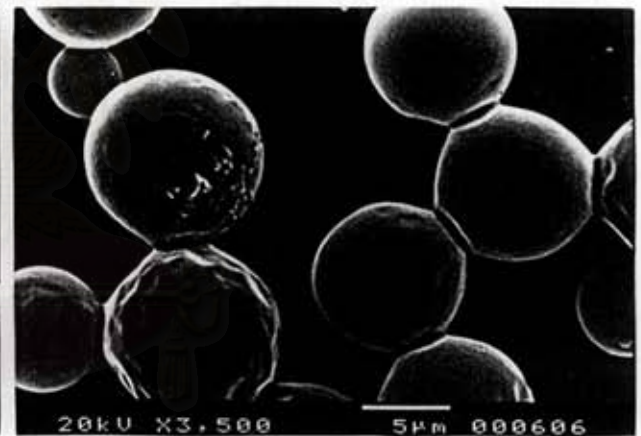

c) Run 604   d) Run 606

Figure 4.15 SEM photographs of poly(styrene-co-2-EHMA) particles by various additives; a) Hexadecane, b) 1-Hexadecanol, c) Methyl palmitate, and d) Bees wax, respectively.
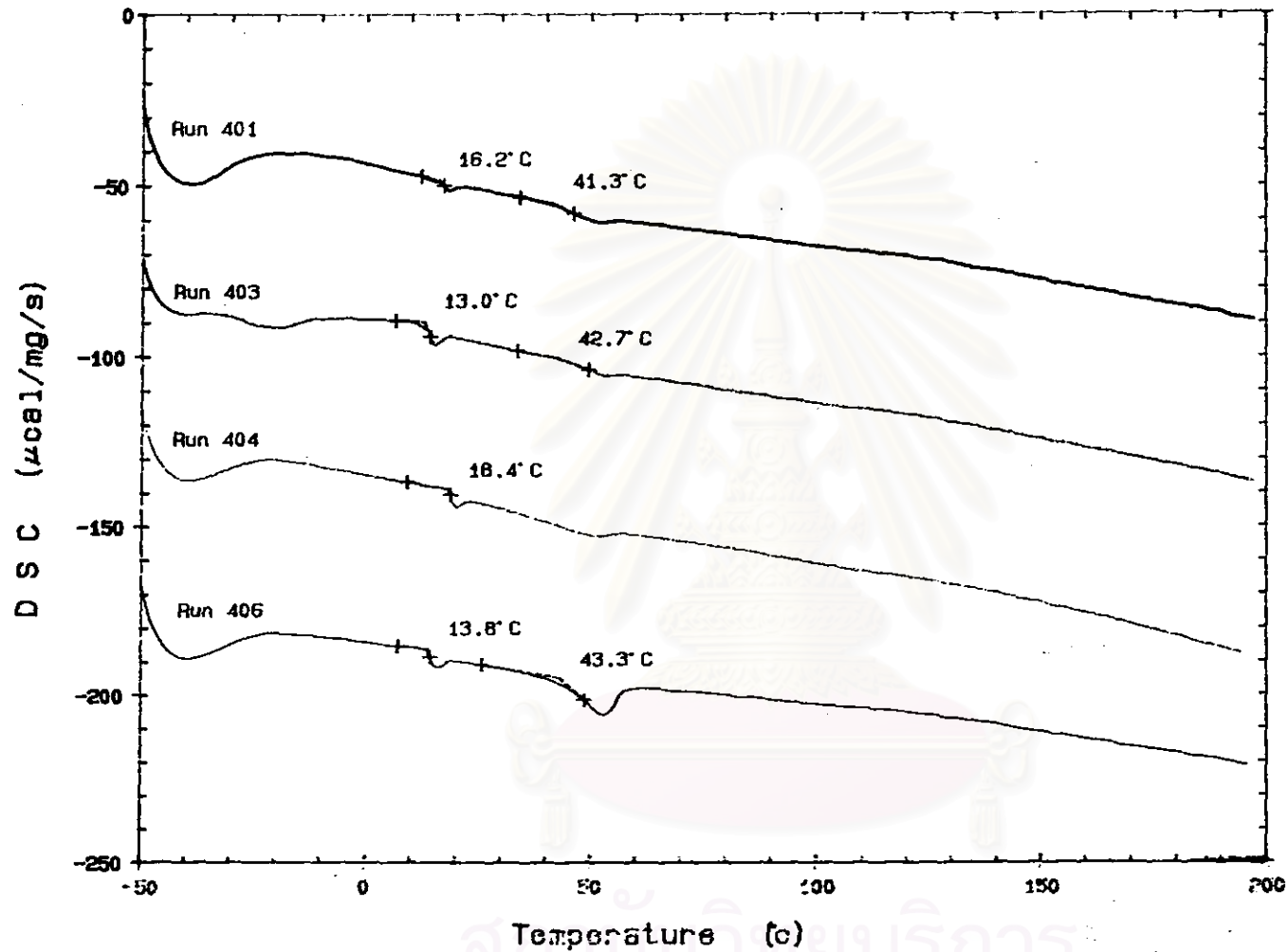
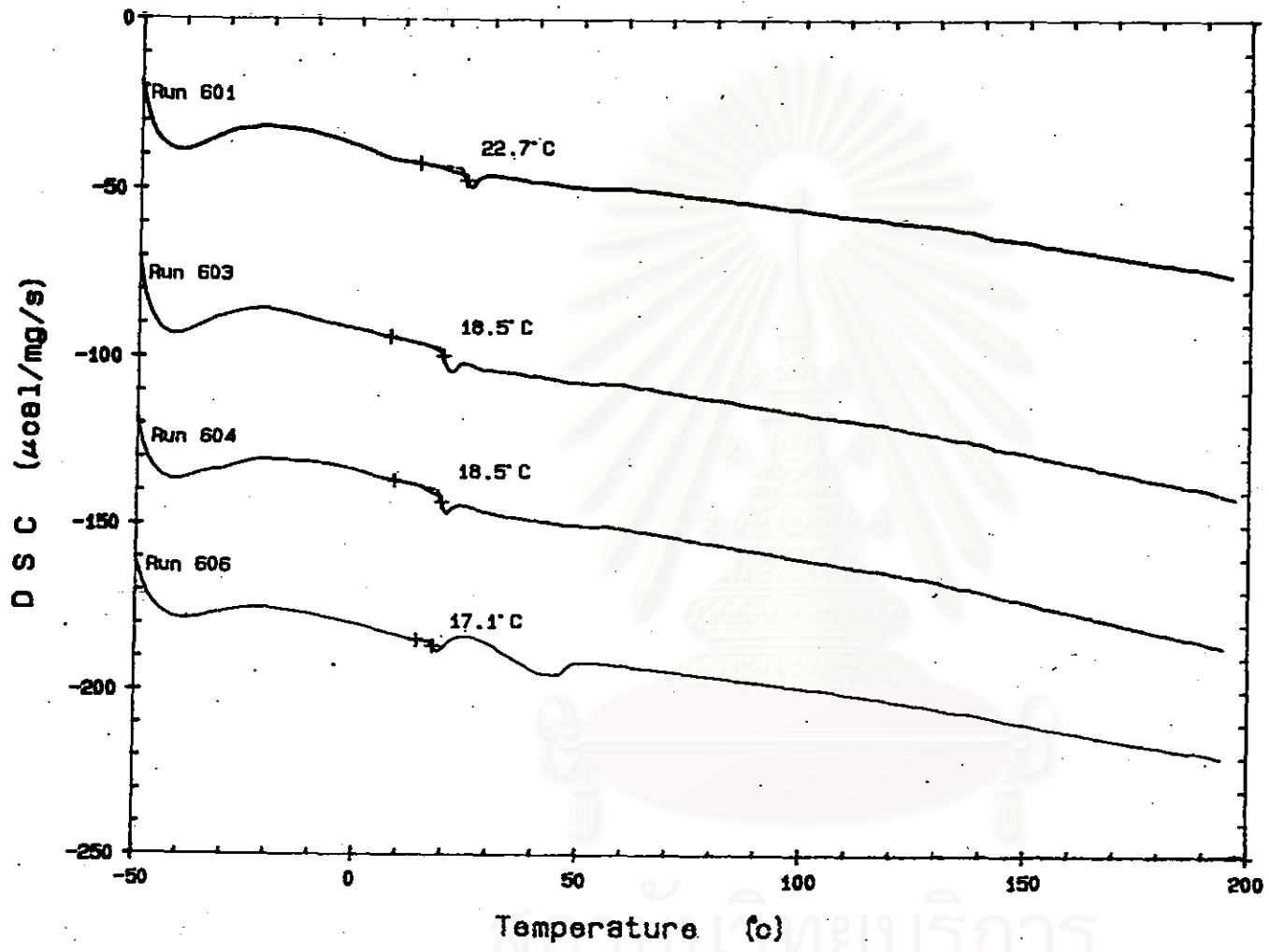**Figure 4.16** DSC curves of poly(styrene-co-n-BMA) weight% ratio of styrene/n-BMA 50:50 in the feed

Figure 4.17 DSC curves of poly(styrene-co-2-EHMA) weight% ratio of styrene/2-EHMA 50:50 in the feed

4.3 Effect of initiator type

The SPG pore size of 0.90 μm was used to prepare the emulsion droplets. The nitrogen pressure at 0.60 Kgf/cm^2 was applied. The dispersion phase containing St-MMA 50:50 weight ratio was studied with different types of initiators namely BPO, AIBN, and ADVN. Table 4.5 gives results of St-MMA copolymer particles synthesized, along with the half-lives ($t_{1/2}$) of the initiator and dissociation rate constant (k_d) at the reaction temperature of 70°C in toluene [39].

Table 4.5 Effect of initiator type on particle size and size distribution, molecular weight and molecular weight distribution of poly(styrene-co-MMA)

Run No.	131	132	134
Initiator	BPO	AIBN	ADVN
k_d(Tol) (s^{-1})	1.1×10^{-5}	4.0×10^{-5}	2.0×10^{-4}
$t_{1/2}$ (Tol) (min)	1049	289	58
Results			
$\overline{D}_e$ (μm)	5.82	6.13	4.85
σ (μm); emulsion	0.68	0.81	0.50
CV (%); emulsion	11.70	13.24	10.37
$\overline{D}_p$ (μm)	5.40	-	3.89
σ (μm); polymer	0.64	-	0.45
CV (%); polymer	11.85	-	11.69
Conversion (%)	48.95	85.66	75.67
$\overline{M}_n$	23100	144500	10950
$\overline{M}_w$	45210	579300	112500
$\overline{M}_w/\overline{M}_n$	1.96[a]	4.90[a]	10.27[b]

Dispersion phase: Styrene 8.00 g, MMA 8.00 g, methyl palmitate 1.50 g, and initiator 0.45 g for all Runs.

Continuous phase: H$_2$O 230 g, PVA-217 1.50 g, SLS 0.04 g, Na$_2$SO$_4$ 0.05 g, hydroquinone 0.016 g. In Run 134, NaNO$_2$ 0.03 g was added in the continuous phase as inhibitor instead of hydroquinone.

[a] unimodal molecular weight distribution

[b] bimodal molecular weight distribution

The droplet and particle size histograms for the St-MMA copolymer with different initiator types are given in Figure 4.18. The addition of methyl palmitate into the dispersion phase, high stability of the emulsion was obtained in all runs. Polymerization with the initiator ADVN, having the fastest decomposition rate (half-life, 58 min), yields a narrow size distribution and gave the smaller particle size diameter. On the other hand, the slow-decomposing initiator BPO (half-life, 1049 min) gives a narrow particle size distribution but has an average droplet size larger than those with ADVN. The sensitivity of particle-size distribution is related to both the decomposition rate of the initiators and the dependence of the particle diameter. This indicates that the fast decomposition rate of the initiator, the oligomers would tend to propagate and form particle nuclei of various chain lengths (mostly short chains). The generation rate probably faster than the rate of stabilizer adsorbed to stabilize them. The shrinkage of particles is thus higher, the histogram in Figure 4.18 in Run 134 tend to separate using ADVN due to the additionally fast-decomposition rate. Whilst, k_d being higher, the radical may escape in the aqueous phase so that part of monomer was used in the process of secondary nucleation. Thus, the particle sizes initiated by ADVN are smaller than what is expected. In contrast, a slow-decomposing initiator generates oligomeric radicals at a much slower rate, for a long period of time results in more uniform chain lengths. Thus, the narrow molecular weight distribution was obtained. GPC chromatogram as shown in Figure 4.19, the molecular weight distribution was examined. The bimodal molecular weight distribution, a weight-average molecular weight polymer ($\overline{M}_w$) higher and broad molecular weight distribution was obtained on the using of ADVN. These indicated the fast decomposition rate results in the generating of oligomer with various chain lengths.

The usage of AIBN as an initiator revealed a different behavior from the others. AIBN, generally regarded as an oil-soluble initiator, is in fact enough soluble in water, and initiated the emulsion polymerization instead of the suspension polymerization. It had been observed previously [40] that oil soluble initiators behave similar to aqueous phase initiators in emulsion polymerization. The evidence is based on the obtained results. As shown in Figure 4.20b, an average particles size lower than 0.1 μm was obtained with high degree of conversion. Considering the monomers present, MMA has a higher water solubility (16.0 g/dm^3) than styrene (0.07 g/dm^3)

[37] so that it can partially dissolve in the aqueous phase. Partitioning of the initiator into the aqueous phase inconsequential due to its low water solubility (< 0.1%). However, increased temperatures and the presence of a surfactant could have a significant effect on AIBN. In the presence of a surfactant, SLS, when the concentration of a surfactant exceeds its critical micelle concentration (CMC), the surfactant molecules aggregate together to form small colloidal cluster referred to as micelles. If the initiator is present in the aqueous phase, the initiating radicals are generated, and diffuse into the micelles. The reaction occurred almost in the micelles and all amount of monomer in the shape of larger droplets is used as reservoir of monomer ($\overline{D}_e$ = 6.13 μm). Furthermore, the emulsion polymerization results in high weight-average molecular weight ($\overline{M}_w$) of 579300, and a broad molecular weight distribution ($\overline{M}_w / \overline{M}_n$) of 4.90 was obtained. As a results, AIBN may not be the good initiator for suspension polymerization [41].
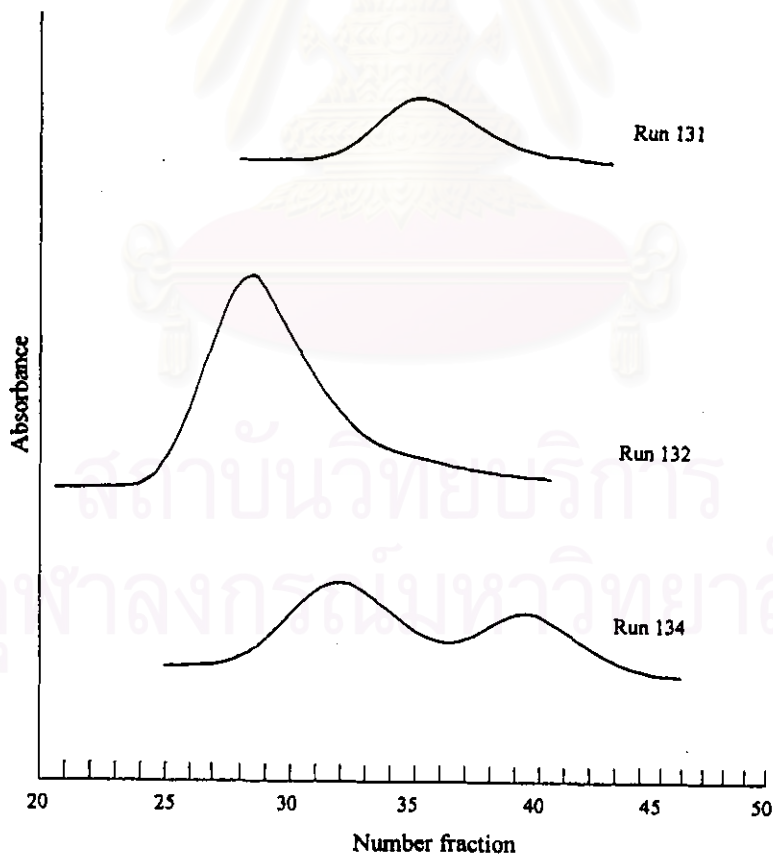

Figure 4.19 GPC chromatogram of poly(styrene-co-MMA); Effect of initiator: a) BPO, b) AIBN, and c) ADVN, respectively.
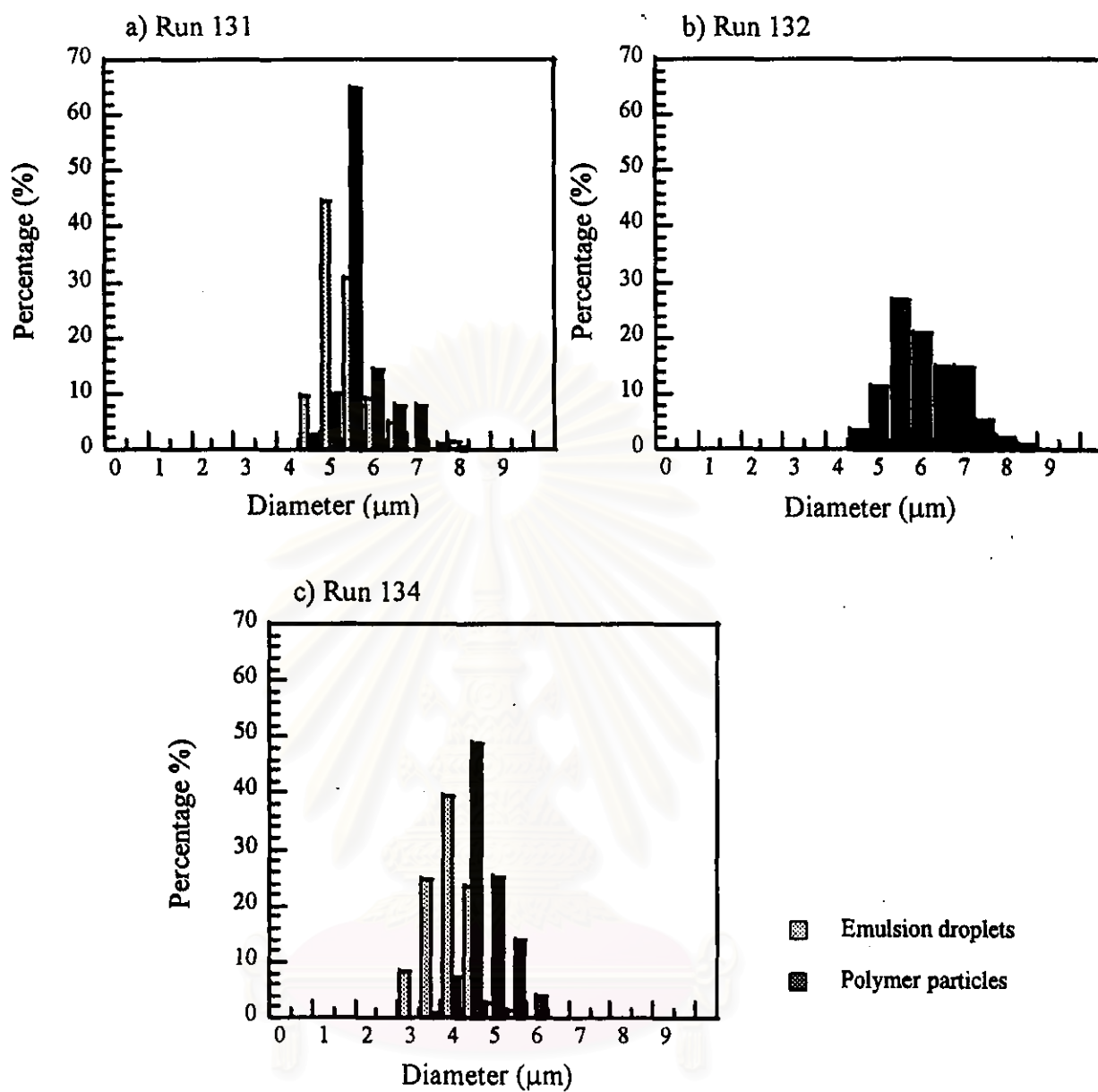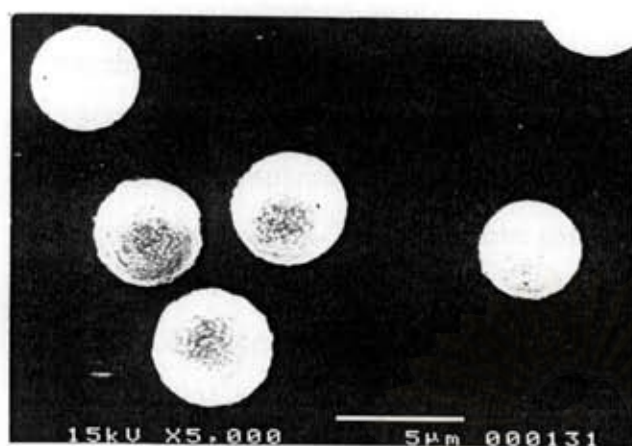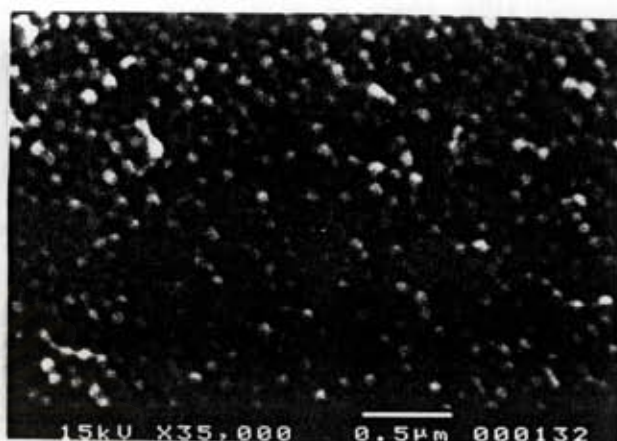
Figure 4.18 Histograms of the size distribution; emulsion droplets and polymer particles; a) BPO, b) AIBN, and c) ADVN, respectively.
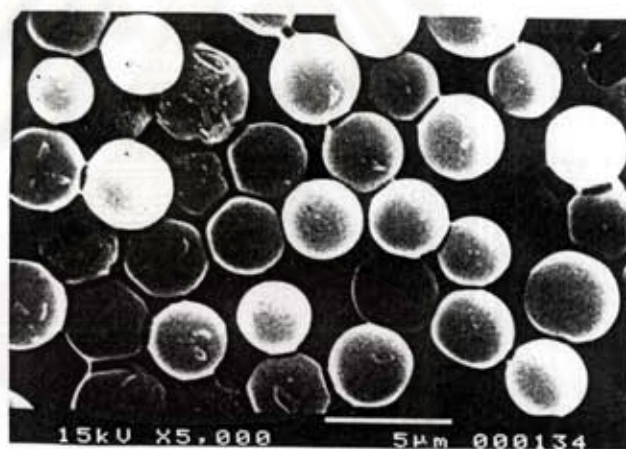
a) Run 131

b) Run 132

c) Run 134

Figure 4.20 SEM photographs of poly(styrene-co-MMA) particles; Effect of initiator: a) BPO, b) AIBN, and c) ADVN, respectively.

4.4 Effect of copolymer composition of poly(styrene-co-MMA)

Poly(styrene-co-methyl methacrylate) particles were prepared using SPG membrane with the pore sizes 1.42 μm. Nitrogen pressure was applied in the range of 0.30-0.34 Kgf/cm^2 to make the emulsion. Polymerization was carried out for 24 h. under N_2 atmosphere at a speed of agitation rate of 180 rpm and polymerization temperature at 75°C. The preparative condition and results are shown in Table 4.6

Table 4.6 Polymerization recipe and experimental results of poly(styrene-co-MMA) particles with various compositions of monomers.

Run No.	130	127	125	126	128
Dispersion phase					
Styrene (g)	16.00	12.00	8.00	4.00	0
MMA (g)	0	4.00	8.00	12.00	16.00
Methyl palmitate (g	1.50	1.50	1.50	1.50	1.50
BPO (g)	0.45	0.45	0.45	0.45	0.45
Results					
Emulsion droplets					
$\overline{D}_e$ (μm)	10.75	10.67	8.93	8.56	6.48
σ (μm)	1.46	1.22	1.23	1.00	0.71
CV (%)	13.57	11.41	13.76	11.73	11.02
Polymer particles					
$\overline{D}_p$ (μm)	7.56	8.76	7.98	8.15	7.86
σ (μm)	1.10	1.21	1.18	1.06	0.93
CV (%)	14.58	13.87	14.80	13.03	11.88
Conversion (%)	43.32	55.84	59.12	66.39	64.72
$\overline{M}_n$	14400	16985	24145	19012	105700
$\overline{M}_w$	33820	36010	59640	46220	514300
$\overline{M}_w/\overline{M}_n$	2.35[a]	2.12[a]	2.47[a]	2.43[a]	4.86[b]
$Tg_{(calcd.)}$	373.0	374.2	375.5	376.7	378.0
$Tg_{(obs.)}$	351.6	360.9	374.4	380.4	380.4

Continuous Phase: H$_2$O 230 g, PVA-217 1.50 g, SLS 0.04 g, Na$_2$SO$_4$ 0.05 g, and hydroquinone 0.016 g. In Run 128, 0.03 g of NaNO$_2$ was added in the continuous phase as inhibitor instead of hydroquinone.

[a] unimodal molecular weight distribution

[b] bimodal molecular weight distribution

4.4.1 Effect of copolymer composition on particle size and particle size distribution of poly(styrene-co-MMA)

Size distributions of emulsion droplets and polymer particles for styrene and methyl methacrylate homopolymer, and St-MMA copolymer are given in Figure 4.21. While the nitrogen pressure was applied in the range of 0.30-0.34 Kgf/cm^2 for each run, the control of pressure certainly reflected the effectiveness of this factor on particle size distribution. The separated histograms were obtained in polystyrene homopolymer in Run 130 and St-MMA copolymer with the ratio of St/MMA of 75:25 in Run 127, respectively. St-MMA copolymer containing 50:50 wt ratio of St/MMA in Run 125 yields an intermediate profile. St-MMA copolymer particles containing 25:75 wt ratio of St/MMA and PMMA homopolymer particles revealed the overlapped histogram in Runs 126 and 128, respectively. On the other hand, the particle diameter decreased with the amounts of MMA were increased. Since Tg of polystyrene and PMMA are almost identical, this may be attributed to the compatibility of methyl palmitate with St-MMA copolymer chains. When the copolymer chains are rich in styrene segments, MP will not mix well with the copolymer chains, leaving a higher interstitial volume in the particles, whilst MMA rich copolymer chains mix well with MP, and a lower interstitial volume will remain.
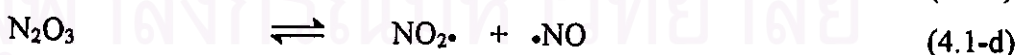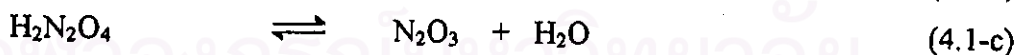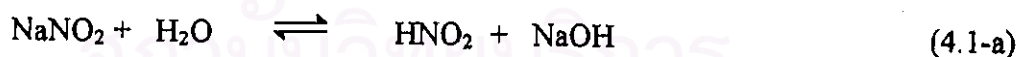
In case of MMA homopolymer, the particle diameter was found larger than emulsion droplets as in Run 128. These appearance possibly occur owing to the properties of MMA. The partially water-soluble MMA polymer was surrounded by water in aqueous phase. As PMMA chains are rather hydrophilic, the particles may contain some water during the polymerization, which behaves like a plasticizer for the chains. During the drying period, the moisture is released and leaves microvoids in the particles. Omi et al. [41] also observed the same phenomenon. Therefore, the volume of polymer particle was increased, resulting in the larger of particle diameter.

4.4.2 Effect of copolymer composition on morphologies of particles

As shown in Figure 4.22, polystyrene homopolymer is spherical in shape. The influence of methyl palmitate as an additive is favorable for styrene polymer. Also, almost all St-MMA copolymers revealed the similar morphologies. The exception is PMMA homopolymer, the particle shape is dented. The low conversion implies that

unreacted monomer remained. During the treatment process, the unreacted monomer is extracted. Thus, the particles with slightly dented area were obtained. The secondary nucleation of the smaller particle on the particles surface was observed and enhanced in case of polystyrene homopolymer and St-MMA copolymer particles, despite the addition of hydroquinone (HQ) in the aqueous phase. An aqueous phase inhibitor, given a task of preventing the secondary nucleation should possess the properties as follows: 1.) eliminate particle formation in the aqueous phase by preventing the propagation of any free radicals in this phase; 2.) inhibitor should not obstruct with polymerization kinetics in the droplets by inducing an induction period, annihilating free radicals; 3.) should not affect the stability of particles [42].

Hydroquinone, a nonelectrolyte compound does not exhibit the electrolyte effect, but HQ causes both an induction period and retardation of the polymerization in oil phase. The partitioning of the inhibitor between the oil and water-phase is responsible for the occurs of secondary nucleation. The inhibiting ability of HQ has been attributed to its oxidated form to quinone, which acts as an inhibitor. If this is the case, then the more oil soluble benzoquinone would likely diffuse to the oil phase. According to this, the extent of secondary nucleation on high content of styrene monomer was increased, creating low molecular weight polymer. To suppress the nucleation of polymer particles in the aqueous phase, sodium nitrite ($NaNO_2$) was used instead of HQ in case of PMMA homopolymer synthesis because HQ causes the coloring of the emulsion. $NaNO_2$ undergoes hydrolysis and forms nitrous acid, which dissociates into nitric oxide and nitric acid as follows [41]:

$$NaNO_2 + H_2O \rightleftharpoons HNO_2 + NaOH \qquad (4.1\text{-}a)$$

$$2HNO_2 \rightleftharpoons H_2N_2O_4 \qquad (4.1\text{-}b)$$

$$H_2N_2O_4 \rightleftharpoons N_2O_3 + H_2O \qquad (4.1\text{-}c)$$

$$N_2O_3 \rightleftharpoons NO_2{\cdot} + {\cdot}NO \qquad (4.1\text{-}d)$$

$$HNO_2 + {\cdot}P \longrightarrow PH + {\cdot}NO_2 \qquad (4.1\text{-}e)$$

$${\cdot}NO_2 + {\cdot}P \longrightarrow P\text{-}NO_2 \qquad (4.1\text{-}f)$$

$${\cdot}NO + {\cdot}P \longrightarrow P\text{-}NO \qquad (4.1\text{-}g)$$

Uneven electrons of nitric oxides and nitrous oxide promote the coupling with polymeric radicals. However, these radicals are also soluble in the oil phase, and inhibit the polymerization to some extent.
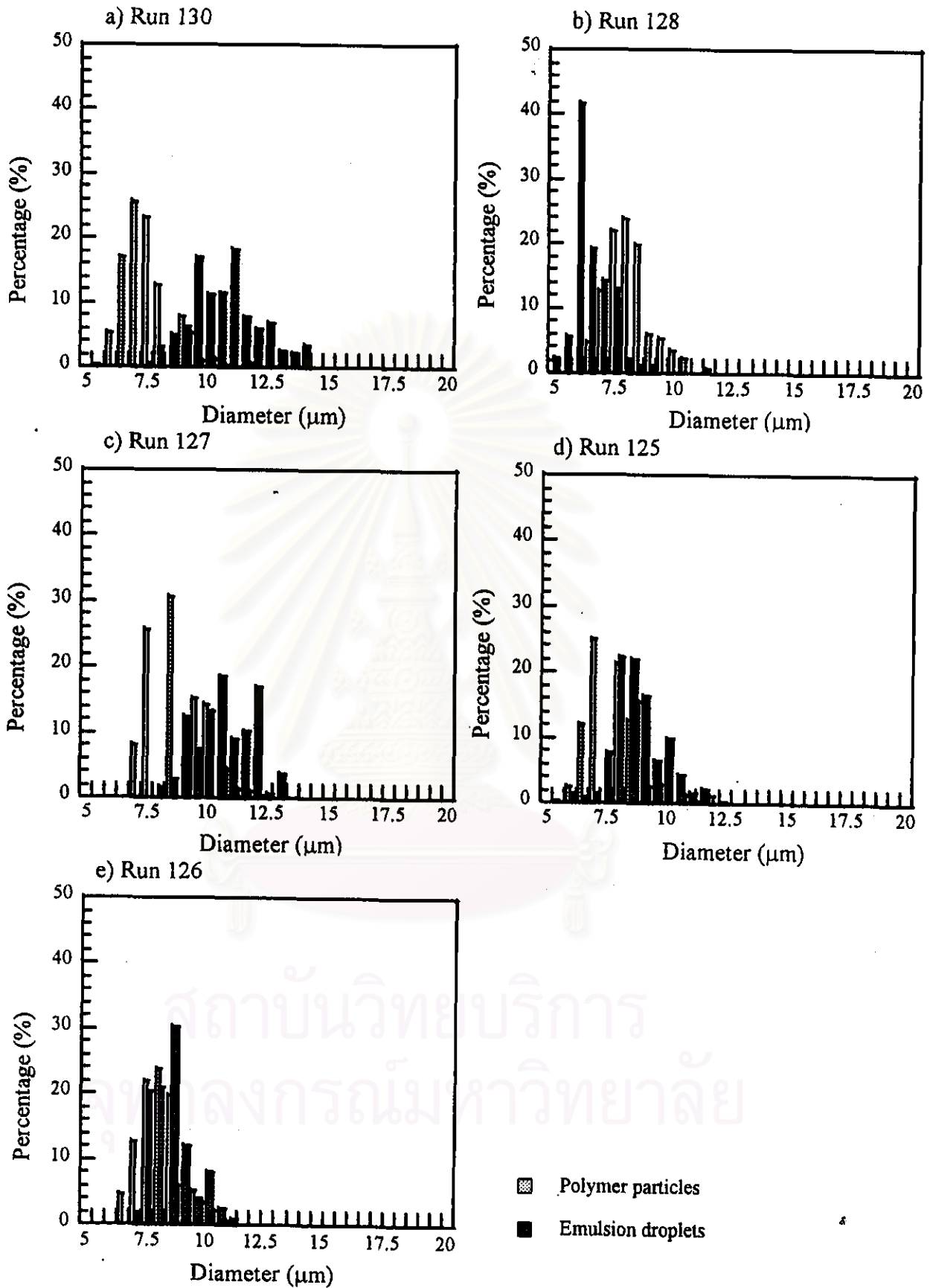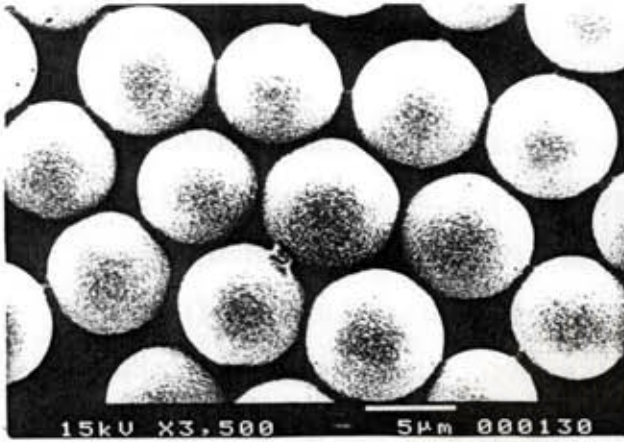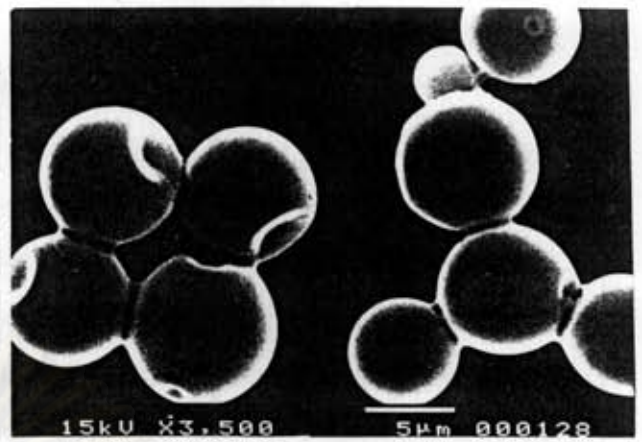
Figure 4.21 Histograms of the size distribution of homopolymer and St-MMA copolymer; Effect of copolymer composition St/MMA in the feed: a) Polystyrene, b) PMMA, c) 75:25, d) 50:50, and e) 25:75 wt% ratio, respectively.
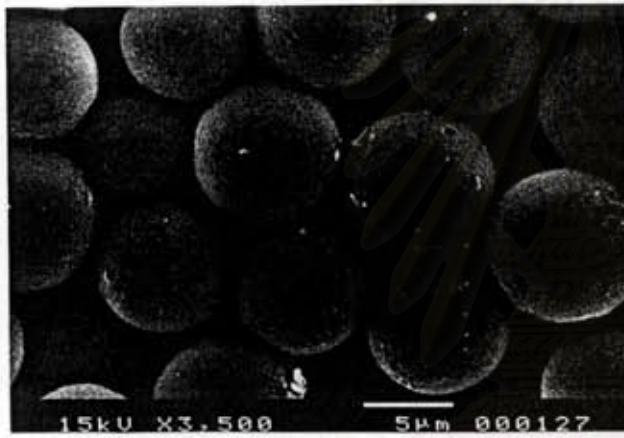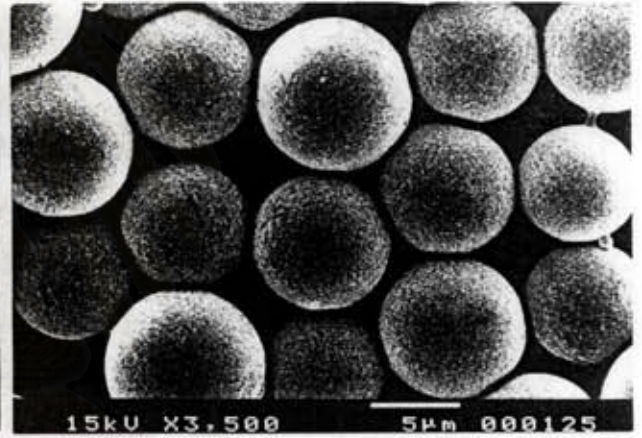
a) Run 130

b) Run 128

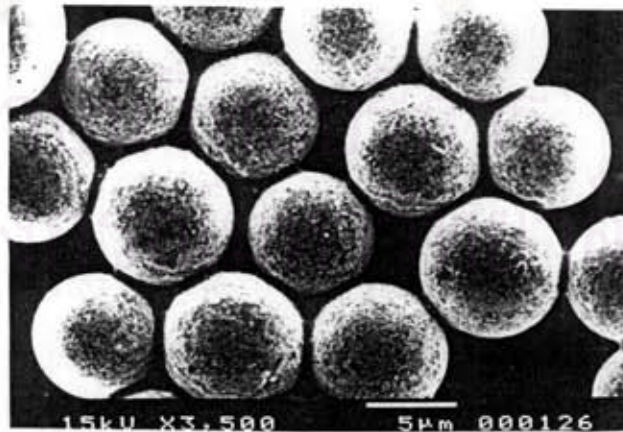c) Run 127

d) Run 125

e) Run 126

Figure 4.22 SEM photographs of homopolymer and St-MMA copolymer particles; Effect of copolymer composition St-MMA in the feed: a) Polystyrene, b) PMMA, c) 75:25, d) 50:50, and e) 25:75 wt% ratio, respectively.

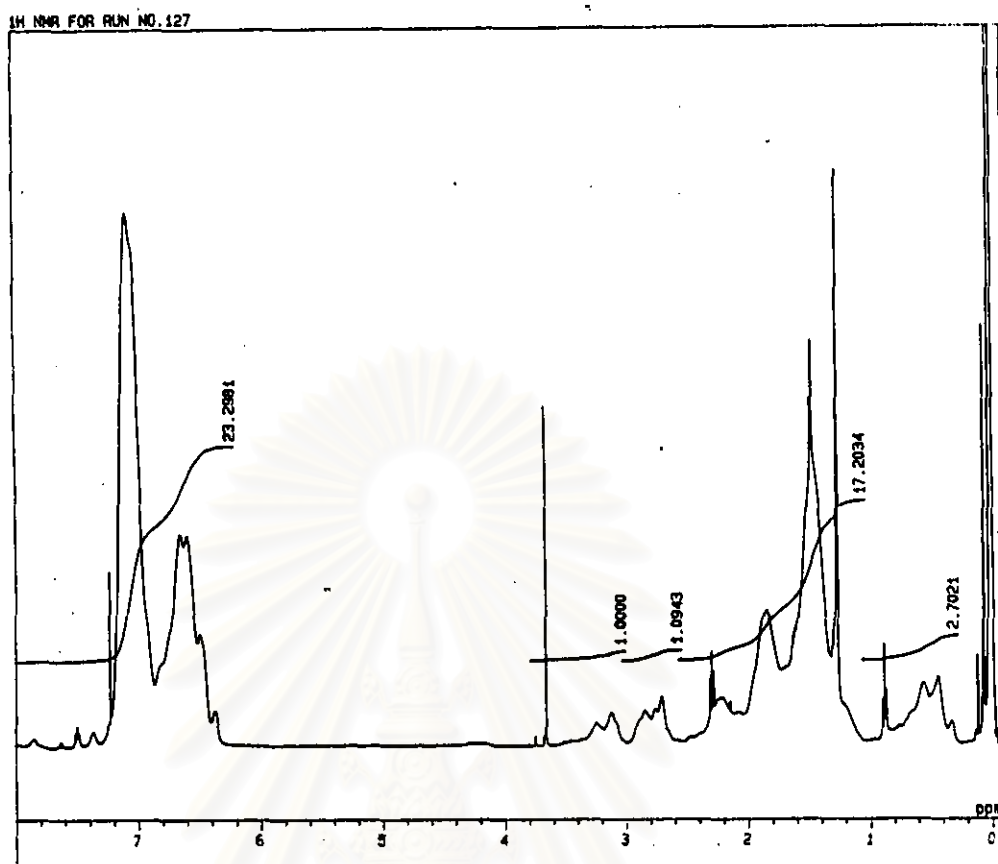### 4.4.3 Microstructure of poly(styrene-co-MMA) using ^{1}H NMR Spectroscopy

A representative ^{1}H NMR spectrum of St-MMA copolymer is shown in Figure 4.23. The resonance signal due to phenyl protons of styrene unit was observed at chemical shift (δ) of 6.3-7.2 ppm. For methyl methacrylate, the methoxy resonance signals, O-CH$_3$, appear in the form of triplet within the wider range of δ 2.2-3.8 ppm resulted from a diamagnetic shielding by the phenyl ring neighboring to the methyl methacrylate group; and the methyl protons, -CH$_3$, appear in the range of δ 0.36-1.1 ppm. The spectral integration of the phenyl and methyl protons was used to determine the copolymer composition because of the large difference in the values of chemical shift for the two kinds of protons. The compositions of St-MMA copolymer are given in Table 4.7

The calculation method for triad distribution based on the equation is which derived in Appendix A, with the reactivity ratio of styrene, γ_S = 0.52 and reactivity ratio of methyl methacrylate, γ_M = 0.46 [39], indicated a tendency towards random copolymer chains. In Figure 4.24, the theoretical triad distribution curves confirm the random character of the monomer placement due to SSS triads growth with a decrease in the mole percent of feed monomer of methyl methacrylate.

Table 4.7 Composition of styrene (f_S), copolymer composition (F_S), and triad relative intensities of poly(styrene-co-MMA)

Run	f_s	f_{MMA}	F_s	F_{MMA}	Relative intensity (from Markov eq.)					
					SSS	SSM	MSM	SMS	MMS	MMM
127	0.7428	0.2572	0.8254	0.1746	0.2409	0.3208	0.1068	0.2155	0.1035	0.0124
125	0.4904	0.5096	0.5038	0.4962	0.2238	0.3011	0.1057	0.1734	0.1658	0.0396
126	0.2429	0.7571	0.3258	0.6792	0.0368	0.1550	0.1631	0.0898	0.3017	0.2536

a)

1H NMR FOR RUN NO.127

123.2981

1.0000

1.0943

17.2034

12.7021

ppm

7   6   5   4   3   2   1   0

b)

1H NMR FOR RUN NO.125

10.6068
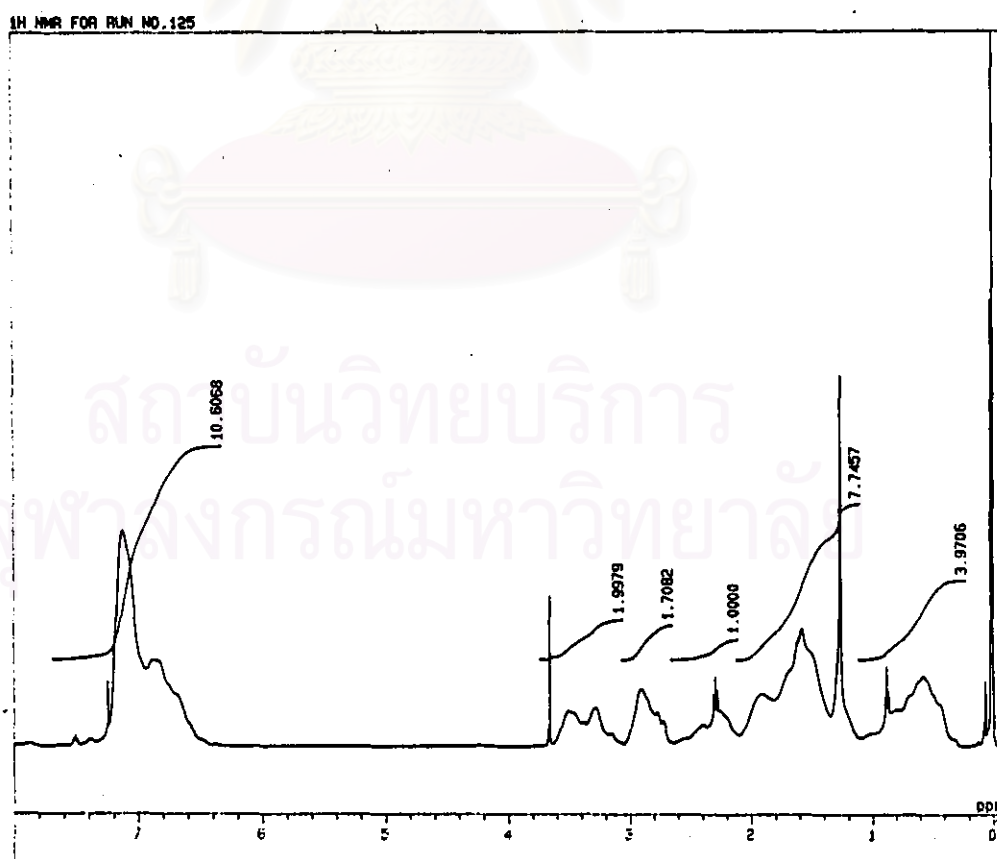
1.9979

1.7082

1.0000

7.7457

3.9706

ppm

7   6   5   4   3   2   1   0

Figure 4.23 ^{1}H NMR spectrum of poly(styrene-co-MMA) weight% ratio of St/MMA in the feed; a) 75:25, b) 50:50

c)

1H NMR FOR RUN NO. 126
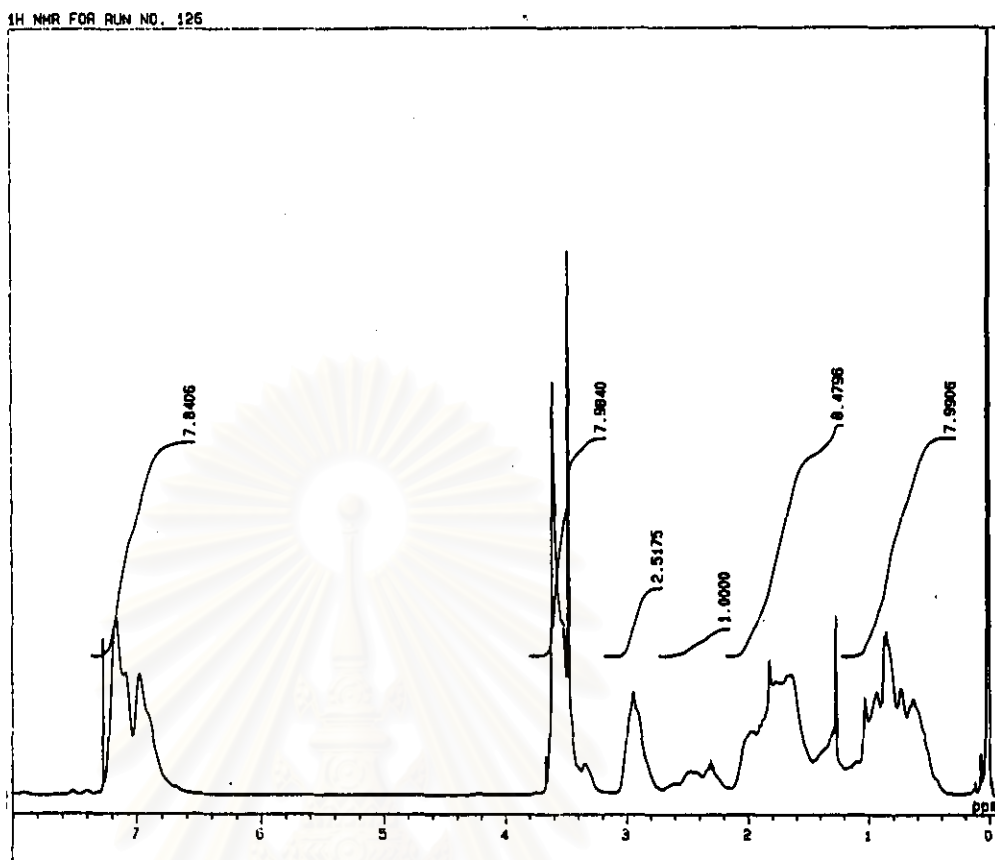
Figure 4.23 (continued) ^{1}H NMR spectrum of poly(styrene-co-MMA) weight% ratio of St/MMA in the feed; c) 25:75.
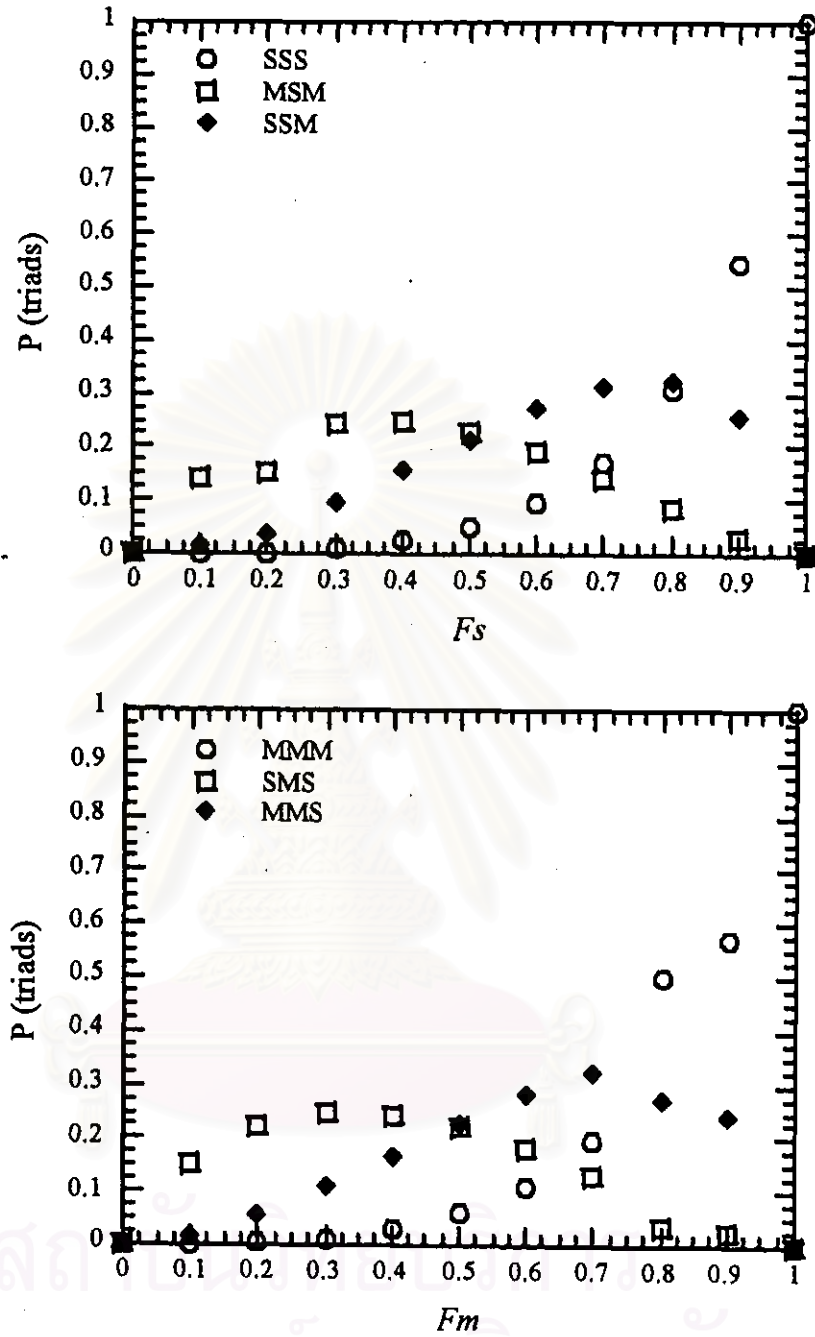
Figure 4.24 Theoretical triad proportions, calculated from Markov equation for St/MMA copolymer

4.4.4 Determination of composition of poly(styrene-co-MMA) by FT-IR spectroscopy

The composition of Styrene and MMA in copolymer can also be calculated from FT-IR spectroscopy. Table 4.8 shows the assignments of FT-IR spectrums and the FT-IR spectrum of homopolymer; and St-MMA copolymer with various ratios of St/MMA is given in Figure 4.25. The assignment of C=O stretching of MMA at 1728 cm^{-1}, and C-H benzene ring stretching of styrene at 698 cm^{-1} were used in quantitative investigation. Both of assignments were clearly observed in all St-MMA copolymers. The peak area of C=O at 1728 cm^{-1} and C-H at 698 cm^{-1} were weighed, the ratio of absorbance (A_{698}/A_{1728}) was calculated, and mole % of styrene in the copolymers was measured which was then compared with the calibration curve [43] in Figure 4.26. The results are shown in Table 4.9.

Table 4.8 Assignment of the FT-IR spectrum of poly(styrene-co-MMA)

Wavenumber (cm^{-1})	Assignment
1728	MMA C=O Stretching
1250-1100	C-O Stretching
990, 755	-COOCH$_3$ Stretching
3061, 3029	Styrene C-H Stretching (benzene ring)
2923, 2851	C-H Stretching (aliphatic)
1602, 1493	C=C Stretching (benzene ring)
760, 700	C-H Out of plane

Table 4.9 Copolymer composition of styrene in the copolymer from FT-IR

Run No.	f_S (mole %)	A_{698}/A_{1728}	F_S (mole %)
127	74.28	0.9748	49.94
125	49.05	0.5068	34.52
126	24.29	0.2156	12.18

The calculated copolymer composition from FT-IR yields an error more than 30% due to the separated assignment in C-H stretch peak. Therefore, the accurate baseline cannot be achieved. However, the FT-IR spectrum reveals in Figures 4.25c, 4.25d, and 4.25e, the peak area of C=O stretching is increased when the quantity of MMA in the feed increases.
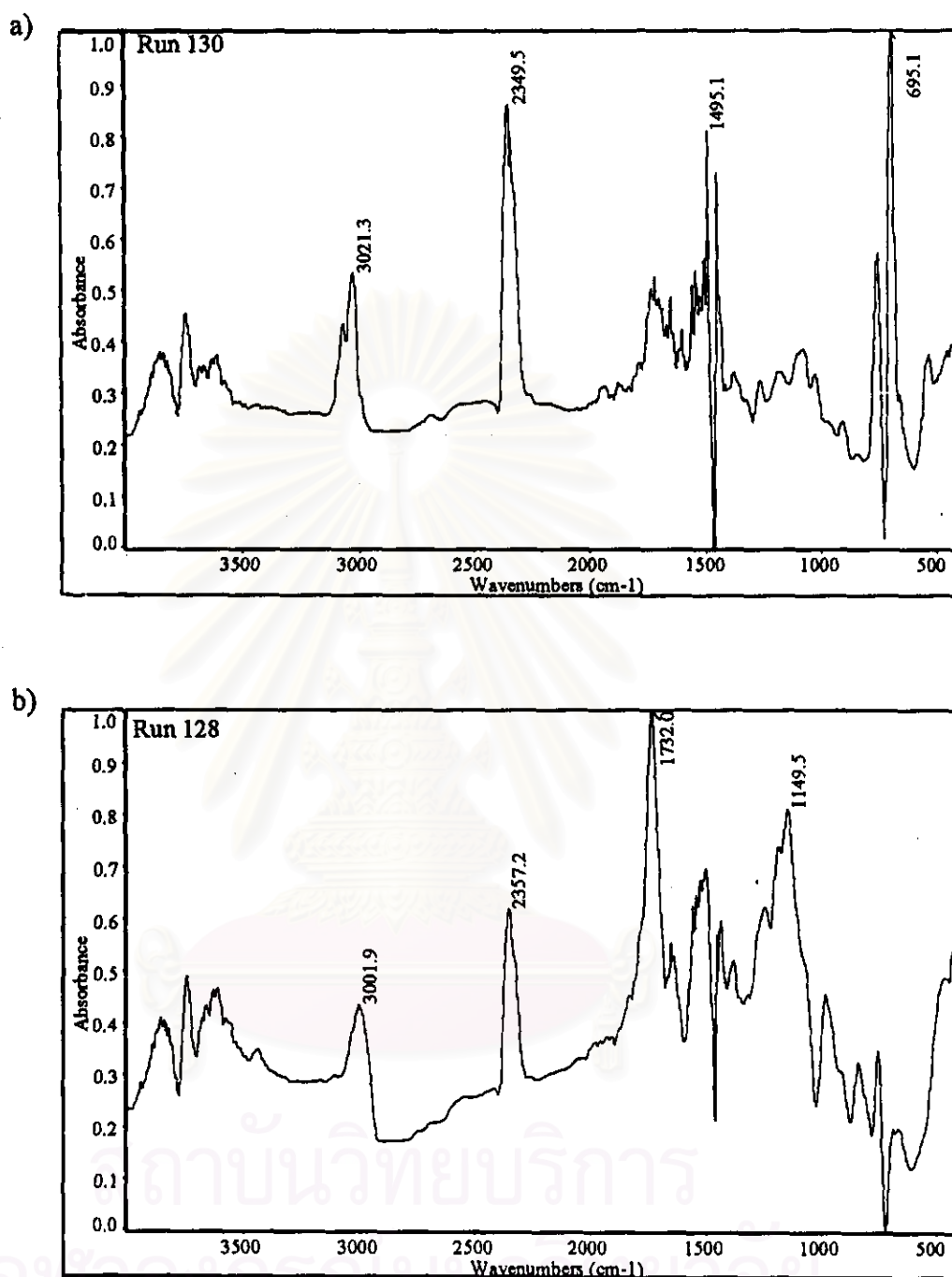
Figure 4.25 FT-IR spectrum of a) polystyrene, b) PMMA homopolymer
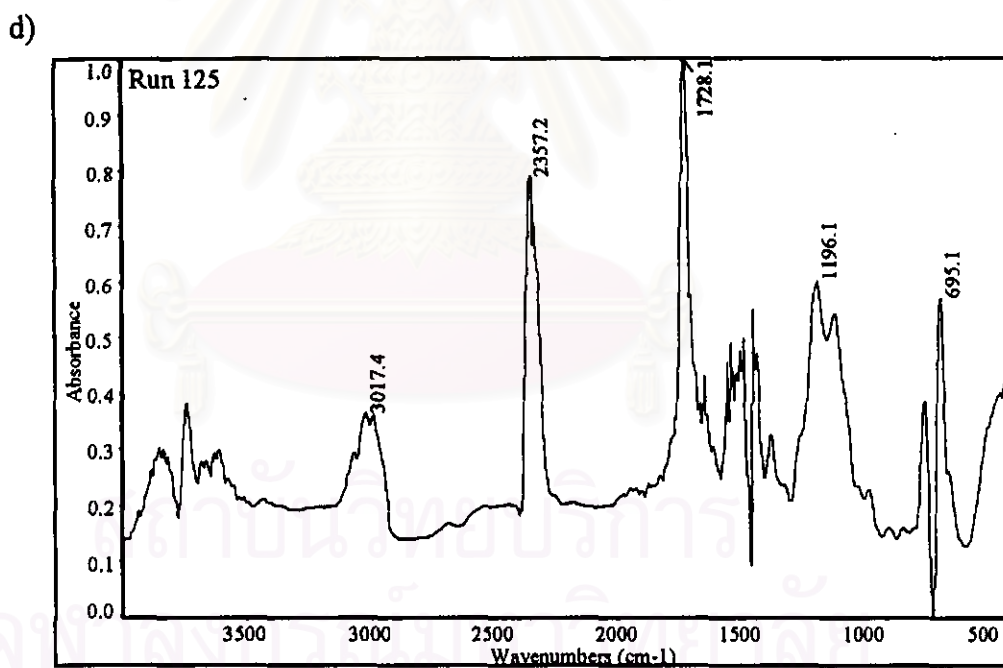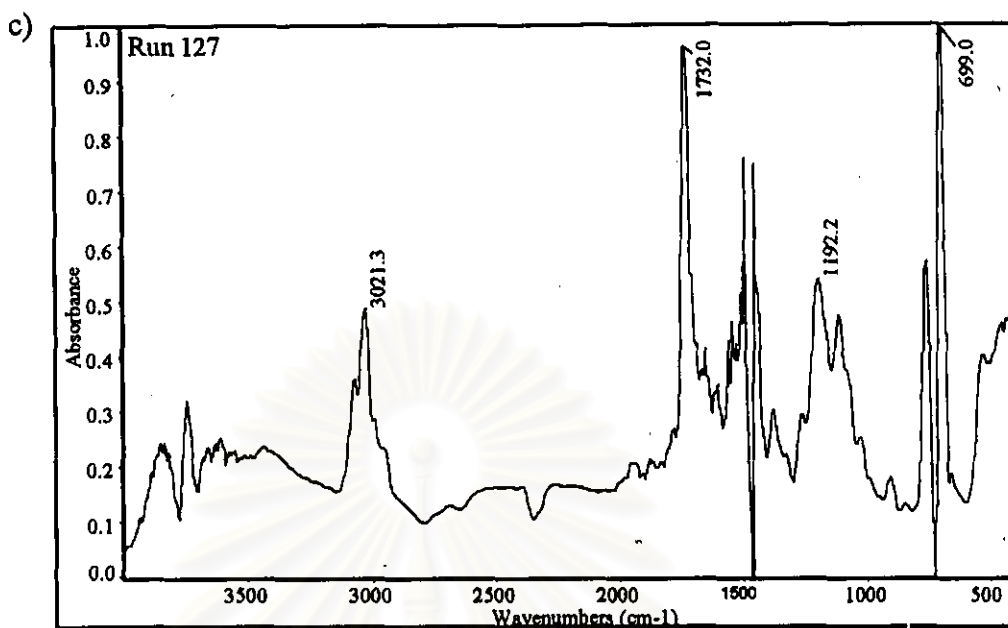
c)

d)

Figure 4.25 (continued) FT-IR spectrum of poly(styrene-co-MMA) weight% ratio of St/MMA in the feed; c) 75:25, d) 50:50
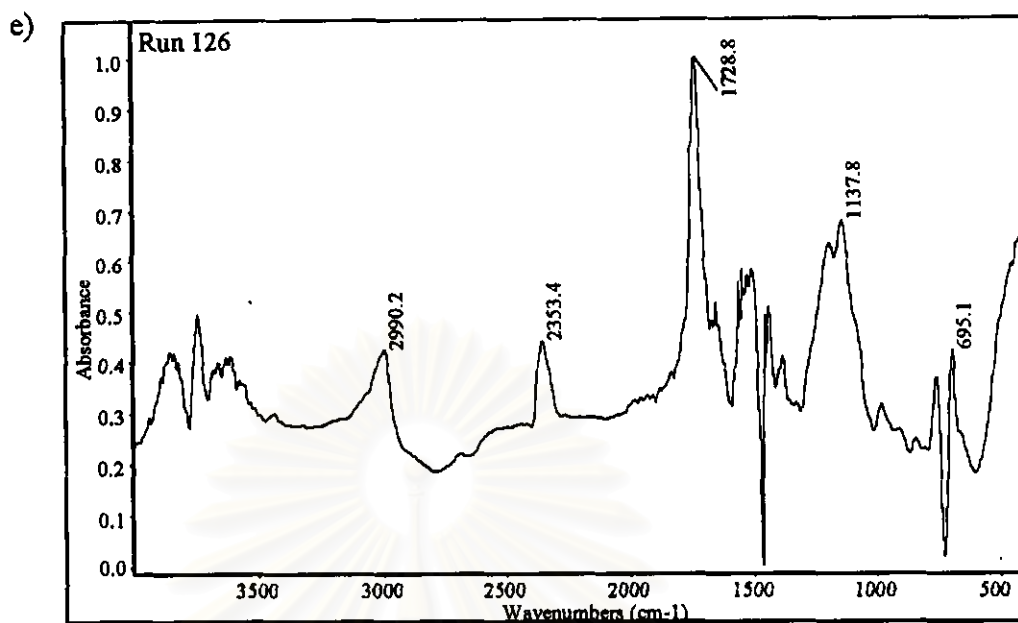
Figure 4.25 (continued) FT-IR spectrum of poly(styrene-co-MMA) weight% ratio of St/MMA in the feed e) 25:75
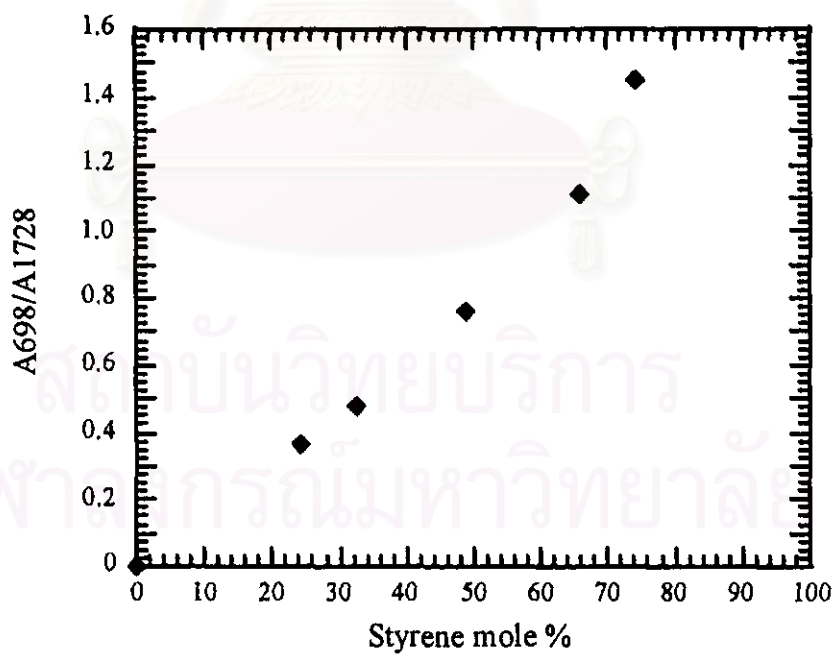

Figure 4.26 FT-IR calibration curve

4.5 Effect of addition monomer

Terpolymerizations of poly(styrene-co-methyl methacrylate-co-n-butyl methacrylate) and poly(styrene-co-methyl methacrylate-co-2-ethylhexyl methacrylate) were studied. The consideration was done based upon the physical properties and chemical properties for the application to dry toner. St-MMA copolymers have higher glass transition temperature than that of the conventional toner. The monomers which provides the lower glass transition temperatures such as n-BMA (Tg = 293 K) and 2EHMA (Tg = 263 K), were used. The first series was studied in case by adding n-BMA into the standard recipe. Dispersion phase thus composed of styrene/MMA/n-BMA weight% ratios of 50:40:10, 50:35:15, 50:30:20, 50:20:30, and 50:10:40 based on monomer concentration were prepared without crosslinking agent. The same recipe and procedure was applied to the preparation of styrene/MMA/2-EHMA. Likewise, methyl palmitate was used as a hydrophobic additive and BPO as an initiator. The emulsion was carried out with the precisely controlled nitrogen pressure for each sample at 0.335 Kgf/cm^2. The preparative conditions and results as given in Table 4.10

4.5.1 Effect of various alkyl methacrylate monomer compositions on particle size and size distribution of the terpolymers

As shown in Figures 4.27 and 4.28, the histogram of size distribution reveals the overlapped profile of emulsion droplets and polymer particles in a similar way in both terpolymer series. In other words, changing the ratio of MMA and n-BMA or 2-EHMA is ineffective on particle size distribution, and the particle sizes in the same range were obtained. Corresponding to the use of alkyl methacrylate, no significant effect arises from the functional group of the monomer.

4.5.2 Effect of various alkyl methacrylate monomer compositions on morphologies

The SEM photographs of the particles of St-MMA-n-BMA terpolymer and St-MMA-2-EHMA terpolymer were given in Figures 4.29 and 4.30, respectively. The morphologies observed reveal that the amount of n-BMA and 2-EHMA influences the

particles formed. In a series of different MMA/n-BMA ratios, while the ratio of n-BMA in terpolymer becomes lower than 40%, the spherical particles were obtained. Difference due to the side chain of MMA and n-BMA are not apparent. When the terpolymer contains 40 wt% n-BMA, the particles were deformed from which each particle sticked closely due to a highly proportion of n-BMA, resulting in the rubber-like morphologies. Consider in case of using 2-EHMA, the deformed particle was found when the composition of 2-EHMA in terpolymer was 20%. The distorted spherical particles connected with thin webs were observed. When the ratio of 2EHMA increased higher than 30%, most particles are distorted and sticked each other. The particles determined from SEM possibly causes an error due to the flatten shape and sticky particles laid on the aluminium stubs surface.

To improve the spheroidal shape of particles, the crosslinking agent was used. The EGDMA in a concentration of 0.1 wt% based on the monomer concentration was added for each St/MMA/n-BMA and St/MMA/2-EHMA ratio. The amount of crosslinking agent based upon the previous experiment was studied on varied concentration of the monomers in St-MMA as discussed in Section 4.1.2, in which highly crosslinked network may cause the phase separation in the previous experiments of St-MMA. Therefore, the low composition of EGDMA was selected so that it can yield lightly crosslinked particles. The polymerization results are shown in Table 4.11. For the system of St/MMA/n-BMA and St/MMA/2-EHMA of weight% ratio, 50:40:10 results in the observed coagulum in both types of terpolymers while this phenomenon does not reveal the crosslinked terpolymer containing alkyl monomer more than 20% of alkyl monomer. The low conversion was resulted, in which predicted the unreacted monomer may enhance the viscosity inside the particle during the polymerization. The terpolymer composed rubbery-like of soft segmental monomer sticks together easily. Thus, the coagulum was naturally occurred.

Table 4.10 Copolymerization recipe and experimental results for non-crosslinked terpolymer poly(styrene-co-MMA-co-n-BMA) and poly(styrene-co MMA-co-2-EHMA)

Run No.	1402	1401	1403	1404	1405	1602	1601	1603	1604	1605
Dispersion phase										
Styrene (g)	8.00	8.00	8.00	8.00	8.00	8.00	8.00	8.00	8.00	8.00
MMA (g)	6.40	5.60	4.80	3.20	1.60	6.40	5.60	4.80	3.20	1.60
nBMA (g)	1.60	2.40	3.20	4.80	6.40	0	0	0	0	0
2EHMA (g)	0	0	0	0	0	1.60	2.40	3.20	4.80	6.40
Methyl palmitate (g)	1.50	1.50	1.50	1.50	1.50	1.50	1.50	1.50	1.50	1.50
BPO (g)	0.45	0.45	0.45	0.45	0.45	0.45	0.45	0.45	0.45	0.45
Results										
Emulsion droplets										
$\overline{D}_e$ (μm)	10.37	9.88	13.68	11.41	12.47	10.82	9.65	12.30	11.52	12.57
σ (μm)	1.62	1.29	1.67	1.55	1.58	1.59	1.07	1.79	1.52	1.50
CV (%)	15.66	13.07	12.24	13.55	12.68	14.73	11.08	14.54	13.23	11.90
Polymer particles										
$\overline{D}_p$ (μm)	7.28	7.93	11.75	9.54	10.19	9.04	7.36	9.54	9.98	13.23
σ (μm)	1.29	1.32	1.53	1.50	1.44	1.40	1.10	1.59	1.20	0.83
CV (%)	17.70	16.67	13.06	15.69	14.14	15.49	15.02	16.69	12.00	6.30
Conversion (%)	36.42	79.26	71.33	66.62	57.62	81.60	50.34	48.84	50.14	69.07
$\overline{M}_n$	23470	23080	24720	26940	22270	16310	21710	19220	22870	23320
$\overline{M}_w$	44330	45810	50170	51440	47970	34300	44920	44000	52710	56020
$\overline{M}_w/\overline{M}_n$	1.89	1.99	2.03	1.91	2.15	2.10	2.07	2.29	2.30	2.40
$Tg_{(calc.)}$, K	364.9	359.9	355.0	345.6	336.7	359.8	352.5	345.5	332.2	319.9
$Tg_{1(obs.)}$, K	-	-	303.0	298.7	300.6	293.2	-	290.4	287.8	316.5
$Tg_{2(obs.)}$, K	352.8	346.6	340.7	332.6	327.3	-	343.6	317.1	-	-

Continuous Phase   H₂O 230 g, PVA-217 1.50 g, SLS 0.04 g, Na₂SO₄ 0.05 g, and hydroquinone 0.016 g.
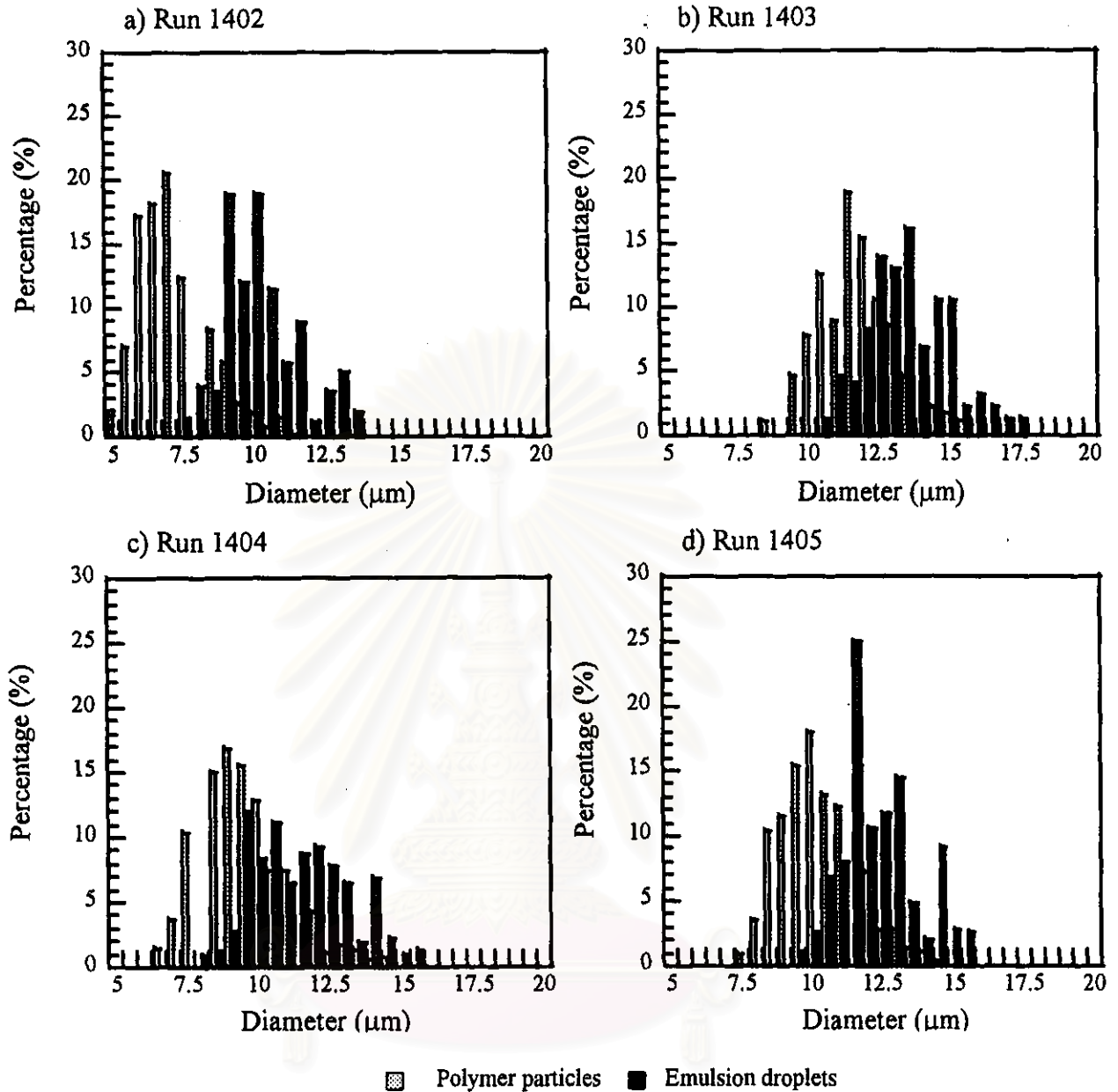
Figure 4.27 Histograms of the size distribution; emulsion droplets and polymer particles; weight fractions of St/MMA/n-BMA in the feed: a) 50:40:10, b) 50:30:20, c) 50:20:30, and d) 50:10:40, respectively.
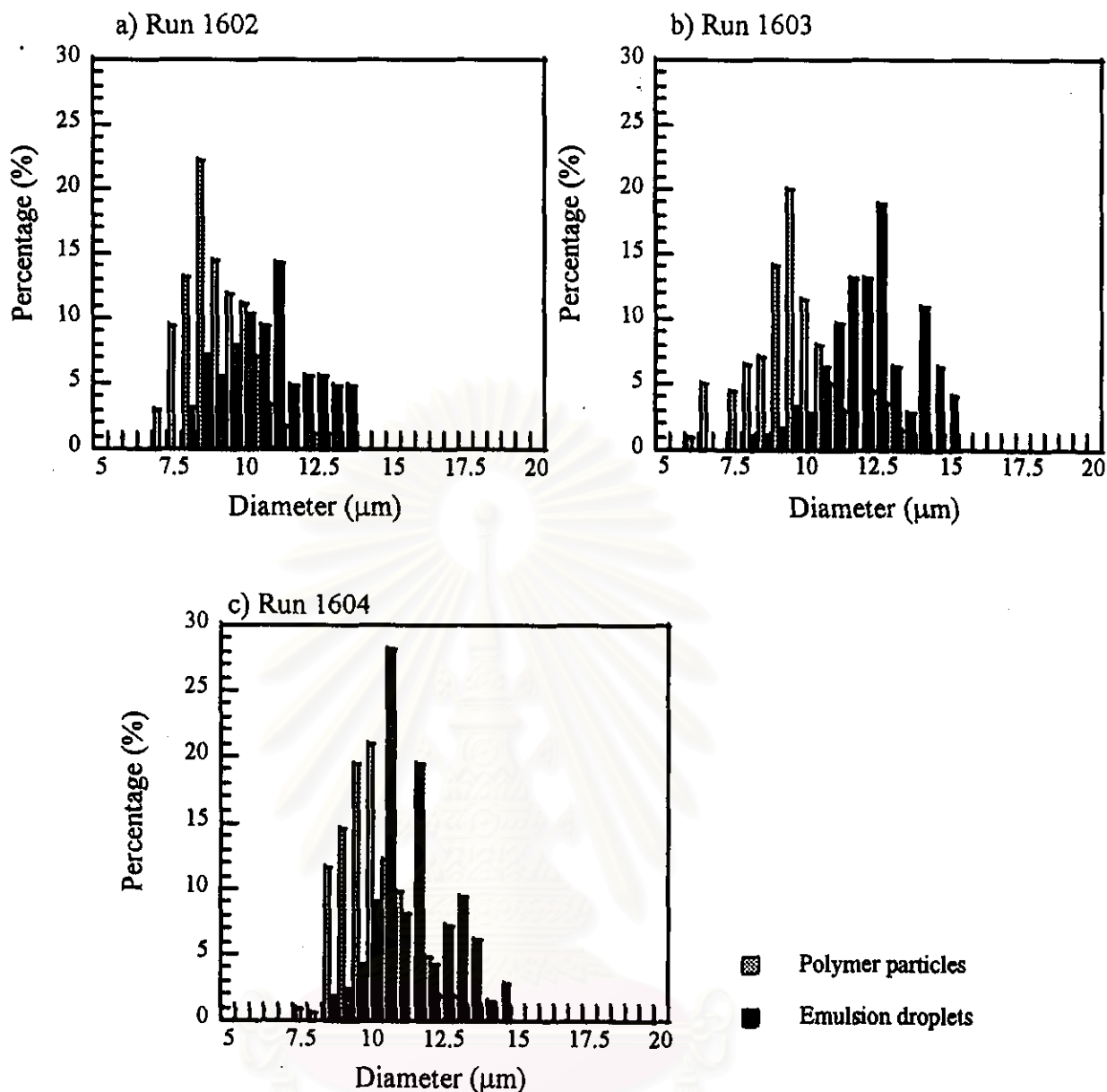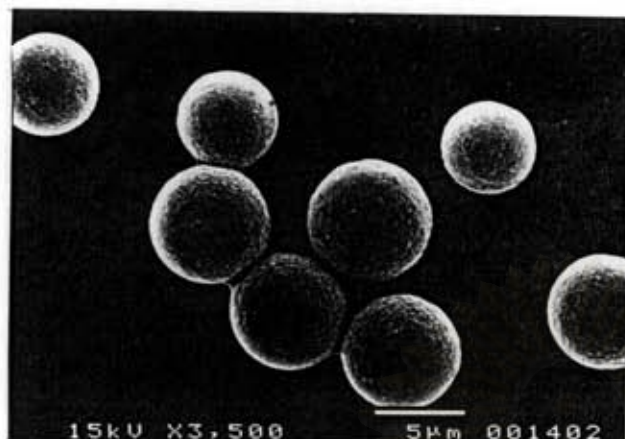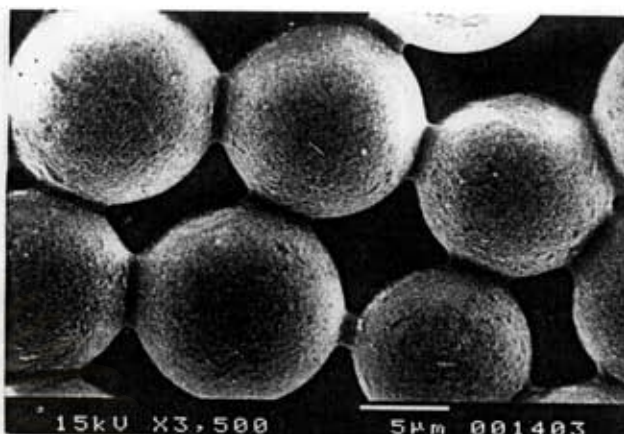
Figure 4.28 Histograms of the size distribution; emulsion droplets and polymer particles; weight ratios of St/MMA/2-EHMA in the feed: a) 50:40:10, b) 50:30:20, and c) 50:20:30, respectively.
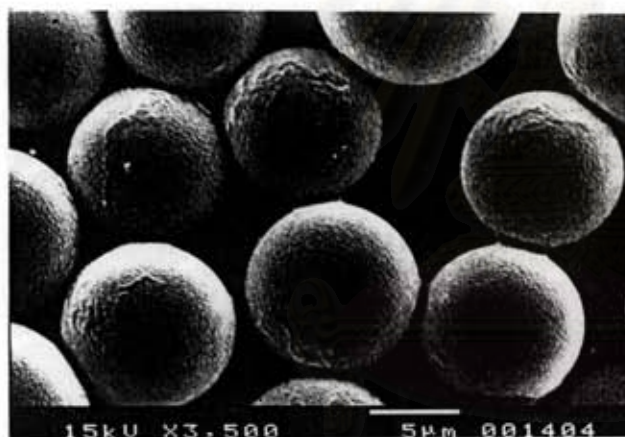
a) Run 1402

b) Run 1403

c) Run 1404

d) Run 1405

Figure 4.29 SEM photographs of poly(styrene-co-MMA co-n-BMA) particles, weight% ratios of St/MMA/n-BMA in the feed; a) 50:40:10, b) 50:30:20, c) 50:20:30, and d) 50:10:40, respectively.
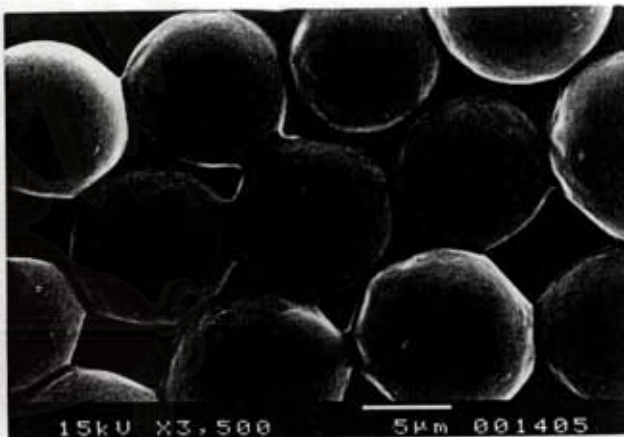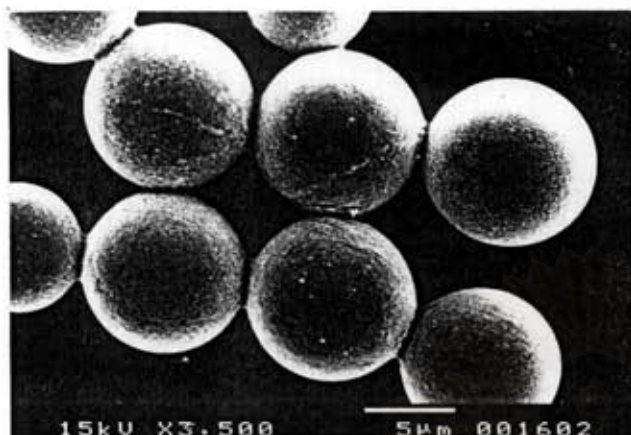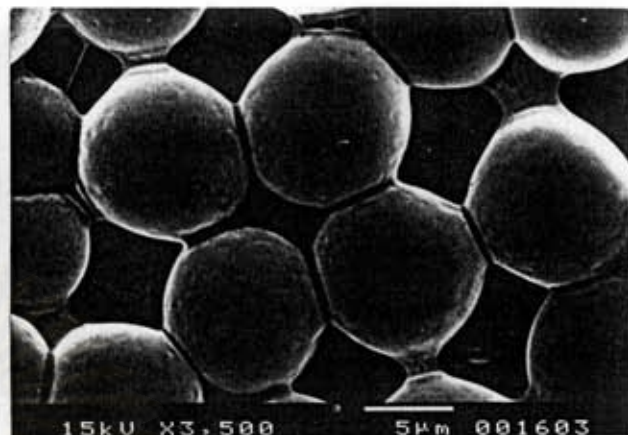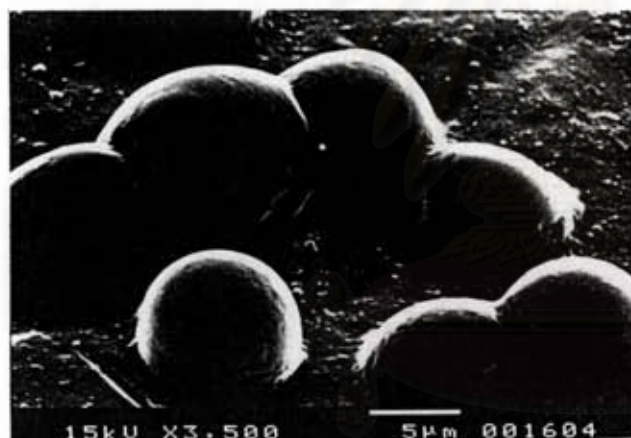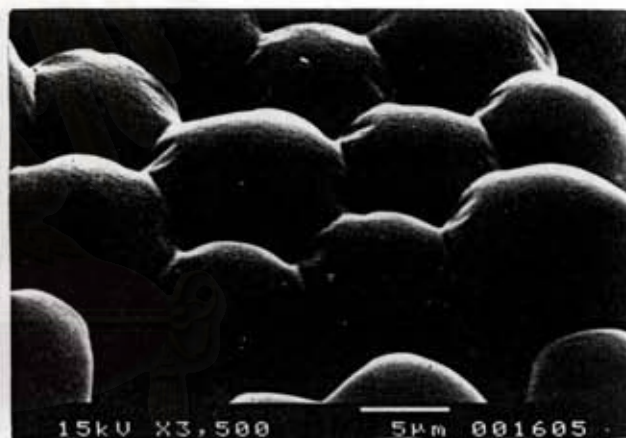
a) Run 1602

b) Run 1603

c) Run 1604

d) Run 1605

Figure 4.30 SEM photographs of poly(styrene-co-MMA-co-2-EHMA) particles, weight ratios of St/MMA/2-EHMA in the feed: a) 50:40:10, b) 50:30:20, c) 50:20:30, and d) 50:10:40, respectively.

Table 4.11 Copolymerization recipe and experimental results for crosslinked terpolymer poly(styrene-co-MMA-co-n-BMA) and poly(styrene-co-2-EHMA)

Run No.	1407	1408	1409	1410	1607	1608	1609	1610
Dispersion phase								
Styrene (g)	8.00	8.00	8.00	8.00	8.00	8.00	8.00	8.00
MMA (g)	6.40	4.80	3.20	1.60	6.40	4.80	3.20	1.60
n-BMA (g)	1.60	3.20	4.80	6.40	0	0	0	0
2-EHMA (g)	0	0	0	0	1.60	3.20	4.80	6.40
EGDMA (g)	0.16	0.16	0.16	0.16	0.16	0.16	0.16	0.16
Results								
Emulsion droplets								
$\overline{D}_e$ (µm)	13.16	13.46	13.67	13.17	12.76	11.62	12.65	12.62
σ (µm)	1.68	1.79	1.55	1.60	1.79	1.40	1.56	1.74
CV (%)	12.73	13.29	11.37	12.12	14.01	12.04	12.30	13.82
Polymer particles								
$\overline{D}_p$ (µm)	coagulum	10.80	11.22	9.96	coagulum	9.55	9.70	10.71
σ (µm)		1.58	1.82	1.36		1.18	1.28	1.60
CV (%)		14.62	16.22	13.63		12.33	13.22	14.94
Conversion (%)	43.86	51.53	55.55	51.22	33.59	59.08	54.09	67.27
$\overline{M}_n$	13900	9413	4435	3788	17150	10510	10860	12810
$\overline{M}_w$	31800	25130	22650	21710	36750	29070	29240	30840
$\overline{M}_w/\overline{M}_n$	5.11	2.67	5.11	5.81	2.14	2.77	2.69	2.44
$T_{g(calcd.)}$, K	359.9	355.0	345.6	336.7	359.9	355.0	345.6	336.7
$T_{g1(obs.)}$, K	285.9	283.9	292.7	288.6	317.7	291.0	299.3	284.8
$T_{g2(obs.)}$, K	344.8	338.1	336.5	325.8	349.7	337.0	333.9	333.9

* Methyl palmitate as additive 1.50 g, and BPO 0.45 g as initiator were added in dispersion phase.
Continuous Phase H_2O 230 g, PVA-217 1.50 g, SLS 0.04 g, Na_2SO_4 0.05 g, and hydroquinone 0.016 g.

4.5.3 Predicted terpolymer composition by ^{1}H NMR

The terpolymer compositions were calculated using the peak area of the $-C_6\underline{H}_5$ (styrene) at chemical shifts (δ) from 6.3 to 7.6 ppm, the peak area of the $-\underline{C}H_3$ (MMA+n-BMA; main chain) and the $-C\underline{H}_2$-$C\underline{H}_2$- (n-BMA; side chain) at δ from 1.1 to 2.6 ppm, and the peak area of the $-C\underline{H}_3$ (n-BMA) at δ from 0.1-1.1 ppm. As briefed in Section 3.3.7, the fraction of styrene in terpolymer can be determined using the following relationship:

Styrene (wt% in terpolymer)

$$= \frac{A(-C_6\underline{H}_5)/5}{A(-C_6\underline{H}_5)/5 + A\left[(-C\underline{H}_3)_{(n-BMA+MMA)} + (-C\underline{H}_2C\underline{H}_2-)_{(n-BMA)}\right]/7 + A(-C\underline{H}_3)/3} \quad (3.6)$$

Results of the calculations are summarized in Table 4.13 for St-MMA-n-BMA terpolymer. In several systems of three monomers, the composition calculated by the terpolymerization model showed a good agreements with the experimentally observed compositions. From these data, the error in the terpolymer composition is estimated at 10% due to the overlapping of the spectra of MMA and n-BMA and uncertainties in division of the integral. Reactivity ratios were obtained from Q-e scheme and the arbitrarily chosen reference values, $Q = 1.0$ and $e = -0.8$ for styrene, $Q = 0.78$ and $e = 0.40$ for MMA, and $Q = 0.82$ and $e = 0.28$ for n-BMA [39]. For St-MMA-2-EHMA terpolymer, the results from ^{1}H NMR is given in Table 4.12. The calculation follows eq. 3.7, the experimentals error was resulted from the overlapped of an assignment of MMA and 2-EHMA as well. Furthermore, the calculation of the composition in St-MMA-2-EHMA was not carried out due to the unsatisfactory data for predicting the reactivity ratio of 2-EHMA.

Styrene (wt% in terpolymer)

$$= \frac{A(-C_6\underline{H}_5)/5}{A(-C_6\underline{H}_5)/5 + A\left[(-C\underline{H}_2)_3C\underline{H}C\underline{H}_2-)_{(2-EHMA)} + (-C\underline{H}_3)_{(MMA)}\right]/12 + A(C\underline{H}_3(C\underline{H}_2)_3-)/6}$$

$$(3.7)$$

Table 4.12 Predicted and experimental composition in radical terpolymerization

	Feed Composition		Terpolymer (mole %)		
				Calculated from	
Run No.	Monomer	Mole %	Exp.	Eq. 39 (Appendix A)	Eq. 41 (Appendix A)
1402	Styrene	50.59	53.12	50.30	49.86
	MMA	42.04	36.51	42.30	41.93
	n-BMA	7.37	10.37	7.40	8.21
1401	Styrene	51.37	50.98	50.67	50.67
	MMA	37.34	36.17	37.87	37.86
	n-BMA	11.24	12.84	11.46	11.46
1403	Styrene	52.21	50.96	50.34	51.10
	MMA	32.52	25.28	32.78	33.28
	n-BMA	15.27	23.76	16.88	15.62
1404	Styrene	53.89	51.09	51.93	52.00
	MMA	22.42	32.18	23.24	23.40
	n-BMA	23.69	16.73	27.04	24.60
1405	Styrene	55.76	49.93	53.00	53.00
	MMA	11.60	23.58	12.38	12.37
	n-BMA	32.63	27.23	34.62	34.63
1602	Styrene	51.65	50.00	-	-
	MMA	42.93	34.00	-	-
	2-EHMA	5.42	15.00	-	-
1601	Styrene	53.06	57.06	-	-
	MMA	38.59	15.76	-	-
	2-EHMA	8.35	27.17	-	-
1603	Styrene	54.55	43.78	-	-
	MMA	34.00	20.65	-	-
	2-EHMA	11.44	35.57	-	-
1604	Styrene	57.79	46.78	-	-
	MMA	24.02	13.13	-	-
	2-EHMA	18.19	39.88	-	-
1605	Styrene	61.44	49.41	-	-
	MMA	12.77	10.86	-	-
	2-EHMA	25.79	39.72	-	-

4.5.4 Effect of various alkyl methacrylate monomer compositions on glass transition temperature

Glass transition temperatures (Tg) of terpolymers were obtained within the range between the values of each homopolymer. The observed Tgs for St-MMA-n-BMA terpolymers are given in Figure 4.31a. The tendency of changing Tg of terpolymer are in a good agreement with the Tg values calculated from Fox's equation, in which the increase of n-BMA resulted in the lower Tg. This terpolymerization may have formed a random terpolymer, with one single Tg approximated equaling to that calculated. However, when the ratio of n-BMA in the terpolymer is higher than 30%, two Tg values were observed. Due to Tg_1 and Tg of n-BMA are closed and Tg_2 approximated by Tg calculation. For the St-MMA-2EHMA, the observed Tg is not in parallel with the calculated curve, and in some cases, two Tgs were observed as shown in Figure 4.31b. The different between the two terpolymer types is probably due to the longer side chain of 2-EHMA in St-MMA-2-EHMA, which hindered the mixing among the terpolymer chains, yielding some inconsistent thermal behavior. This tendency was found in the crosslinked terpolymer of both St-MMA-n-BMA and St-MMA-2-EHMA also. The observed Tgs of the crosslinked terpolymer are shown in Figure 4.32a and 4.32b.
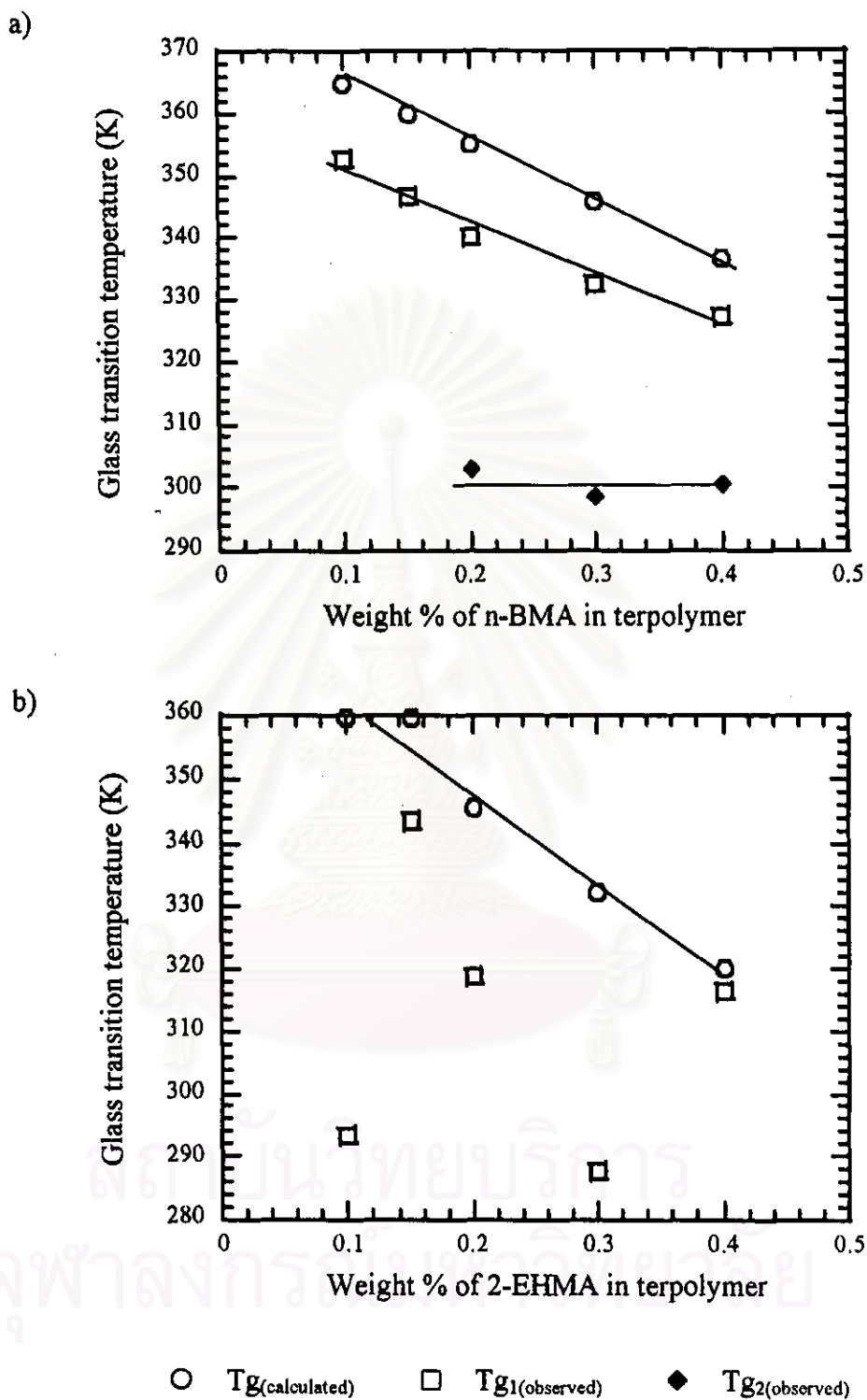
a)

b)

○ Tg(calculated)   □ Tg1(observed)   ◆ Tg2(observed)

Figure 4.31 Relationship between Tg of noncrosslinked terpolymer with various compositions of monomer: a) poly(styrene-co-MMA-co-n-BMA), and b) poly(styrene-co-MMA-co-2-EHMA).
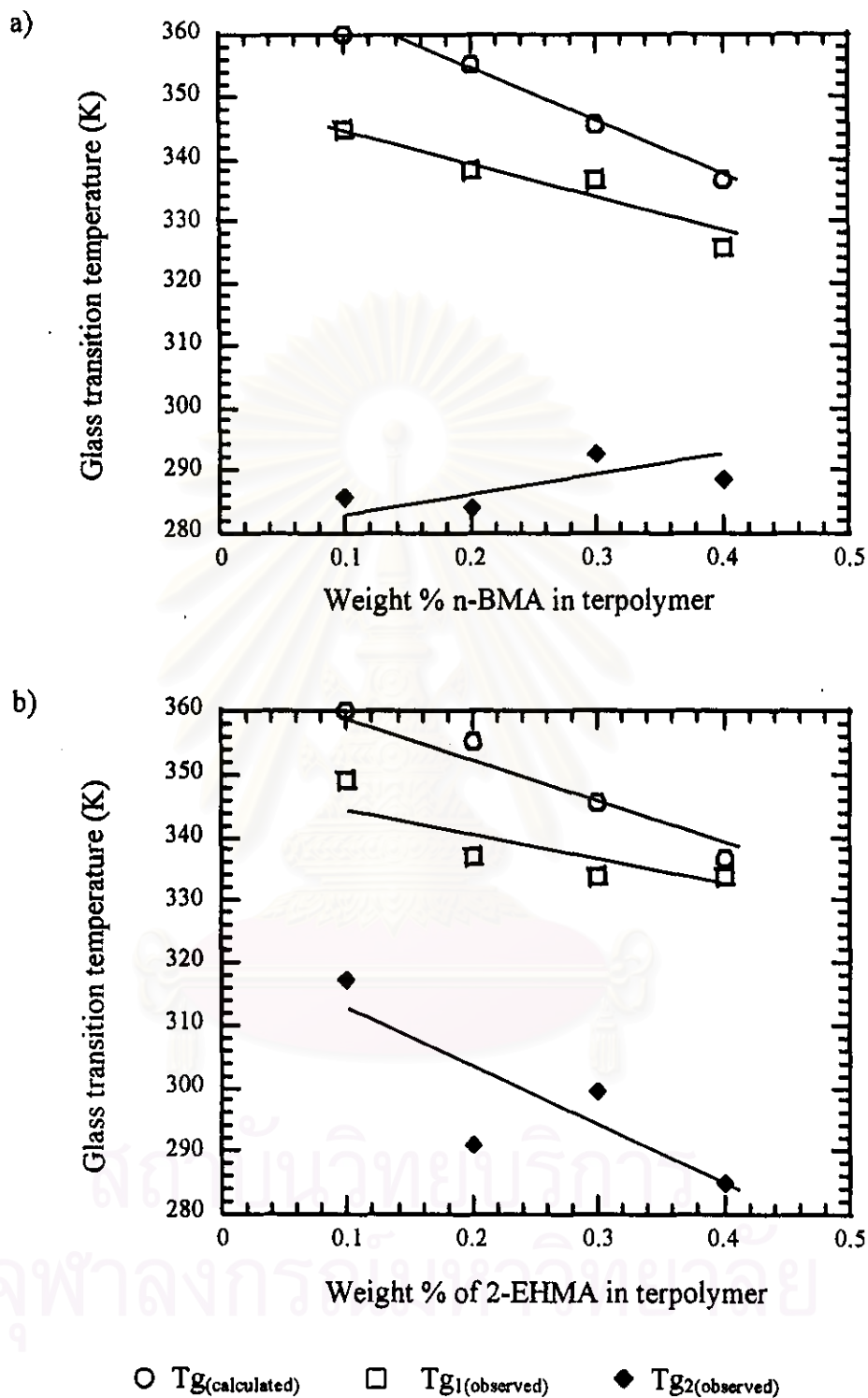
Figure 4.32 Relationship between Tg of crosslinked terpolymer with various compositions of monomer:a) poly(styrene-co-MMA-co-n-BMA), and b) poly(styrene-co-MMA-co-2-EHMA).